



ENGINEERING-PDH.com
ONLINE CONTINUING EDUCATION

BUILDING ENVELOPE INVESTIGATION USING LIDAR SCANNING

Main Category:	HVAC Engineering
Sub Category:	-
Course #:	HVC-116
Course Content:	43 pgs
PDH/CE Hours:	3

OFFICIAL COURSE/EXAM
(SEE INSTRUCTIONS ON NEXT PAGE)

WWW.ENGINEERING-PDH.COM

TOLL FREE (US & CA): 1-833-ENGR-PDH (1-833-364-7734)

SUPPORT@ENGINEERING-PDH.COM

HVC-116 EXAM PREVIEW

- TAKE EXAM! -

Instructions:

- At your convenience and own pace, review the course material below. When ready, click “Take Exam!” above to complete the live graded exam. (Note it may take a few seconds for the link to pull up the exam.) You will be able to re-take the exam as many times as needed to pass.
- Upon a satisfactory completion of the course exam, which is a score of 70% or better, you will be provided with your course completion certificate. Be sure to download and print your certificates to keep for your records.

Exam Preview:

1. While the lidar scanner, which uses online-waveform processing to capture multiple returns per pulse, is capable of successfully capturing focus surfaces through snowfall, the TIR sensor does not perform well.
 - a. True
 - b. False
2. For coincident internal temperature measurements, a set of Onset HOBO UA-002-64 pendant loggers were used for multiple temperature logging locations within the buildings. These low-cost, small-footprint sensors have a measurement range of -20°C to ___ $^{\circ}\text{C}$, an accuracy of $\pm 0.53^{\circ}\text{C}$, and a resolution of 0.14°C at 25°C .
 - a. 30
 - b. 50
 - c. 70
 - d. 100
3. The lidar sensor is a Riegl VZ-1000 terrestrial laser scanner (TLS). It uses a 1550 nm eye-safe pulsed laser to measure range and surface reflectance values over a 360° horizontal by ___ $^{\circ}$ vertical field of view.
 - a. 75
 - b. 80
 - c. 90
 - d. 100
4. Subsequent scans around the buildings were tied to the baseline georeferenced scan through two processes: coarse registration and Multi Station Adjustment (MSA).
 - a. True
 - b. False

5. The FLIR SC640 has similar technical specifications to the VarioCAM HD 880 sensor, with the following main differences: spectral range of 7.5–13 μm , 640×480 pixel image, measurement range of -40°C to ____ $^\circ\text{C}$, measurement accuracy of $\pm 2^\circ\text{C}$ or $\pm 2\%$ of the reading, and operating temperature range of -15°C to 50°C .
 - a. 1100
 - b. 1300
 - c. 1500
 - d. 1700
6. As per the Palmer Station Master Plan, USAP is assessing the infrastructure for modernization to allow the station to be a viable platform for Ant-arctic research for the next _____ years.
 - a. 15 to 30
 - b. 25 to 40
 - c. 35 to 50
 - d. 40 to 65
7. According to the reference material, coarse registration involves finding a minimum of ____ common points between overlapping scans to roughly align the point clouds together.
 - a. 2
 - b. 4
 - c. 6
 - d. 8
8. According to the DWR section in the reference material, the black-trim windows displayed large temperature anomalies, whereas the all-trim windows displayed little to no heat loss below their frames.
 - a. True
 - b. False
9. Which of the following facilities had a significantly lower temperature differential between its exterior surfaces and therefore a more uniform temperature gradient when observing the thermal envelope 3-D model?
 - a. CRREL
 - b. Biolab
 - c. GWR
 - d. Terralab
10. The TIR sensor outputs a proprietary-format image file for each image captured. This file type, .irb, is then ingested into InfraTec's IRBIS 3 software package for both analysis and processing.
 - a. True
 - b. False

Abstract

Through the use of an integrated lidar and thermal infrared (TIR) ground-based sensor, the Cold Regions Research and Engineering Lab (CRREL) conducted a survey at Palmer Station, Antarctica, in October 2015 to assess thermal building envelopes of the main infrastructure. These co-registered data produce three-dimensional models with assigned temperature values of target buildings, useful in spatially identifying thermal anomalies and areas for potential improvements in building construction (e.g., insulation, soffits, windows, doors, etc.). For Palmer Station, the National Science Foundation identified three focus buildings: Biolab, Garage-Warehouse-Recreation (GWR), and Terralab. The lidar/TIR data collection was conducted in tandem with interior and exterior temperature and atmospheric measurement logging, handheld thermal and electro-optical imagery collection, and Global Navigation Satellite System (GNSS) real-time kinematic surveys to place the collected data in a global coordinate system.

This report details the findings of these efforts and summarizes the results for each of the three focus buildings. In general, the more recently constructed Terralab exhibits a sounder building envelope without any major thermal deficiencies when compared to both the Biolab and GWR buildings. The three-dimensional models of all buildings allow for a holistic view of these thermal deficiencies and provide a means for prioritizing potential construction activities.

Contents

Abstract	ii
Figures and Tables.....	iv
Preface.....	vi
Acronyms and Abbreviations.....	vii
Unit Conversion Factors	viii
1 Introduction.....	1
1.1 Background.....	1
1.2 Objectives.....	2
1.3 Approach	3
1.4 Instrumentation platform: lidar/TIR system.....	4
2 Data Acquisition.....	7
2.1 Interior temperature loggers	7
2.2 Exterior climate station data	9
2.3 GNSS RTK control survey	10
2.4 TIR handheld imagery.....	12
2.5 Electro-optical (EO) imagery	13
2.6 Lidar/TIR system acquisition	13
3 Data Processing.....	17
3.1 Lidar registration/georeferencing.....	17
3.2 Temperature value registration.....	18
4 Results and Discussion.....	19
4.1 Biolab	19
4.2 GWR.....	22
4.3 Terralab	25
5 Conclusions.....	28
References	29
Appendix A: Palmer Survey Maps.....	30
Appendix B: CRREL Lidar/TIR System Data Acquisition Procedure	33
Appendix C: Scanning Log—Reflector Survey	35
Report Documentation Page	

Figures and Tables

Figures

1	Site layout for Palmer Station, Antarctica, with the three surveyed buildings (Biolab, Garage-Warehouse-Recreation, and Terralab) identified	3
2	CRREL's lidar/TIR system in use on the GWR rooftop platform, October 2015. The InfraTec VarioCAM HD camera is mounted to a Riegl VZ-1000 terrestrial laser scanner	4
3	Sample TIR image captured by the VarioCAM sensor	6
4	Internal building temperatures from various locations within each of the three buildings at the time of external lidar and thermal scanning.....	8
5	Palmer Station temperature climatology	9
6	For the dates of deployment, Palmer Station daily temperature and temperature climatology.....	10
7	Example image of a 10 cm reflector cylinder with a reflective tape face used in georeferencing lidar point clouds.....	11
8	CRREL's Dr. Elias Deeb operating the FLIR SC640 during daytime for comparison to nighttime image collections.....	13
9	CRREL's Adam LeWinter collecting data at Palmer Station using the lidar/TIR System	14
10	Comparison of lidar data collected without snow precipitation (<i>top</i>) and with significant falling and blowing snow, highlighted by reflectance, in <i>red (bottom)</i> . While the lidar system is capable of measuring the building surface through snowfall, the building surface resolution is reduced, and the thermal values are skewed	16
11	Detail of damaged or unseated insulation along southwest roofline soffits on the Biolab. Multiple areas were completely devoid of this insulation material	19
12	Southwest face of Biolab. Significant venting of heat was observed at the ground-level doorway, along the lower connection of the cafeteria deck, at the cafeteria deck exit, and along the roofline soffit. In addition, degradation of insulation is evident below the upper-level windows.....	20
13	Ground-level entrance and vestibule on the south-southwest section of Biolab. Higher surface temperatures were measured at the entrance and within the vestibule. The second- and third-level soffits show heat loss. Some heat loss was observed along exterior metal sheeting overlaps	20
14	Southeast face of Biolab, including the walkway and entrance into the kitchen/cafeteria. Significant heat loss was observed along the top soffit with the highest temperature values measured on far right side of the image. Windows display varying levels of heat loss. There is degradation of insulation below the upper windows, possibly from water leaking. The ceiling level of the ground level/floor of second level has heat loss along the exterior.....	21
15	Southeast face of Biolab. The far right of the roofline shows significant heat loss along the roofline soffit. There is degradation of insulation below upper windows, possibly due to water leaking. The ceiling of the ground level and floor of the second level has heat loss along the exterior. A hot spot is visible to the right of the kitchen exhaust vent.....	21

16 South face of GWR. There is significant degradation below white-trim windows. Smaller, black-trim windows display no leaking of heat below the frames, indicating a better seal. Heat loss is observed along the roofline soffit, though not as large of a temperature difference compared to observations of the Biolab soffits. Lower portions of the building were obstructed by heavy equipment parked by the building, a necessity for charging and heating purposes22

17 Detail images from the south face of GWR. The *top* image, captured with the handheld DSLR camera, demonstrates the two main types of windows in use in GWR: black-trim and white-trim. The white-trim windows clearly show significant heat loss below while no temperature differences were measured below the smaller black-trim windows.....23

18 East face of GWR, displaying significant heat loss and insulation damage below white-trim windows. The damage to insulation continues from the top-floor windows fully down to ground level. A patched panel to the right of the windows also displays heat loss below. No significant heat loss was measured along the roofline or exterior panel seams.....24

19 Significant heat loss below all windows along the GWR north side. All windows are white-trim style25

20 Interior scan of the garage bay in GWR. The *top* image is a two-dimensional view of the point cloud colored by surface reflectance in the lidar laser wavelength (dark-to-light equals low-to-high surface reflectance). The bottom image is the same view colored by temperature. An even gradient from the floor up in temperature is visible along with areas of cold ingress and heat loss around the garage door and entry doorway.....25

21 Visible image (*top*) and lidar/TIR image (*bottom*) of Terralab. Small temperature gradients along the exterior panel seams are visible. The most significant heat loss occurs at the entryway doors and a vent halfway up the image foreground support post. Overall, this building appears sufficiently insulated.....26

22 Temperature-colored point cloud view of the southeast side of Terralab.....27

23 Panorama of the interior of Terralab’s south room. Slight cool air ingress is visible along the wall–ceiling interface. Studs and rafters are visible through the drywall. Of note is the minimal cool air ingress along all of the windows, indicating that they are performing very well.....27

24 Screen shot of the lidar/TIR survey data for the three major buildings at Palmer Station, Antarctica, in the web-based portal.....28

Tables

1 Lidar and thermal acquisition dates/times at Palmer Station.....10

2 Recorded values from the RTK surveys of the 10 cm reflector cylinders used for georeferencing the lidar point clouds12

Preface

This study was conducted for the National Science Foundation, Office of Polar Programs (NSF-OPP), under Engineering for Polar Operations, Logistics, and Research (EPOLAR) EP-ANT-15-31, “Building Envelope Assessment Using Thermal Infrared and Lidar Scanning.” The technical monitor was Ms. Margaret Knuth, Program Manager, NSF-OPP, U.S. Antarctic Program.

The work was performed by the Lidar and Wetlands Group of the Remote Sensing/GIS Center of Expertise (CEERD-RS), U.S. Army Engineer Research and Development Center, Cold Regions Research and Engineering Laboratory (ERDC-CRREL). At the time of publication, Dr. Elias Deeb was lead for the Lidar and Wetlands Group; Mr. David Finnegan was Chief, CEERD-RS; and Ms. Janet Hardy was the program manager for EPOLAR. The Deputy Director of ERDC-CRREL was Mr. David B. Ringelberg, and the Director was Dr. Joseph L. Corriveau.

COL Bryan S. Green was Commander of ERDC, and Dr. David W. Pittman was the Director.

Acronyms and Abbreviations

CAD	Computer-Aided Design
CRREL	U.S. Army Cold Regions Research and Engineering Laboratory
EO	Electro-Optical
ERDC	Engineer Research and Development Center
GNSS	Global Navigation Satellite System
GWR	Garage-Warehouse-Recreation
LTER	Long-Term Ecological Research
MSA	Multi Station Adjustment
NSF	National Science Foundation
OPP	Office of Polar Programs
RTK	Real-Time Kinematic
3-D	Three-Dimensional
TLS	Terrestrial Laser Scanner
TIR	Thermal Infrared
USAP	U.S. Antarctic Program

Unit Conversion Factors

Multiply	By	To Obtain
bars	100	kilopascals
degrees (angle)	0.01745329	radians
degrees Fahrenheit	$(F-32)/1.8$	degrees Celsius
feet	0.3048	meters
inches	0.0254	meters
microinches	0.0254	micrometers
microns	1.0 E-06	meters
miles (U.S. statute)	1,609.347	meters
miles per hour	0.44704	meters per second
pounds (mass)	0.45359237	kilograms
yards	0.9144	meters

1 Introduction

1.1 Background

As identified in the U.S. Antarctic Program (USAP) Blue Ribbon Panel (2012), energy efficiency of building infrastructure plays a significant role for the U.S. Antarctic Program (USAP) in operations at remote stations, such as Palmer Station, Antarctica (located on the south side of Anvers Island, off the west coast of the Antarctic Peninsula [$64^{\circ}46'27.72''$ S, $64^{\circ}3'13.81''$ W]), and directly relates to fuel consumption and cost. In practice, thermography, or thermal imaging, is a nondestructive method to quickly and accurately identify variations within the building envelope contributing to heat loss. Additionally, lidar is a convenient data collection and surveying tool that is useful in creating three-dimensional (3-D) models.

This effort deploys a capability developed at the U.S. Army Cold Regions Research and Engineering Laboratory (CRREL) that combines both thermal infrared (TIR) and lidar scanning as a comprehensive tool for assessing building envelopes. The resulting 3-D model, which includes both the thermal signature of the building along with its relative location in space, may be combined with existing engineering drawings to develop a more complete solution for evaluating and prioritizing energy improvements. Through this, decision makers can use the detailed building envelope information in context with proposed construction activities and overall site master planning.

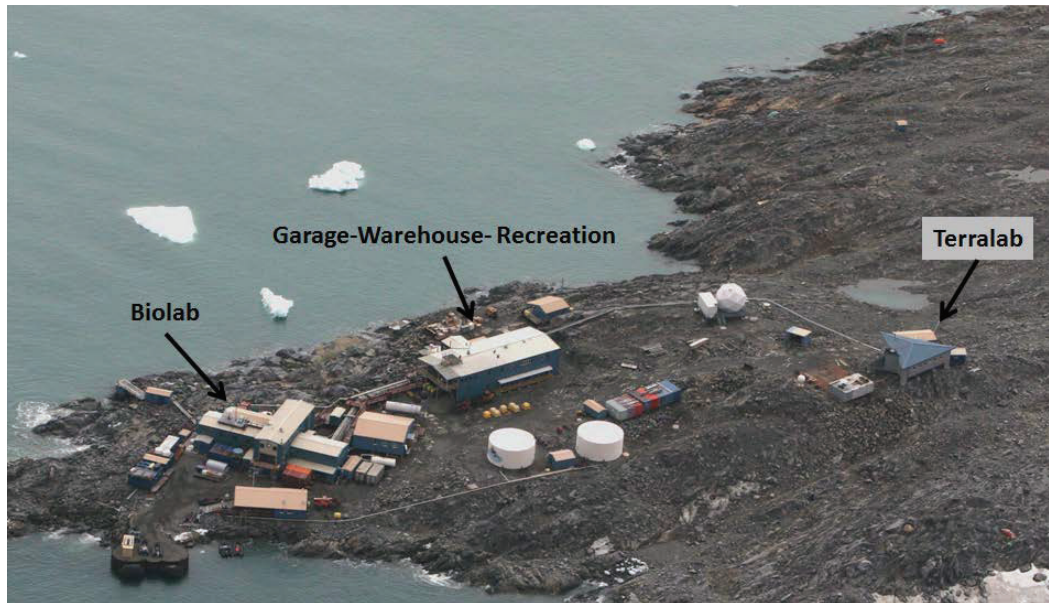
Several previous activities by CRREL have addressed building envelope assessments, including a study of the Big House at Summit Station, Greenland (Barna et al. 2011); an infrared survey of the South Pole Elevated Station (Phetteplace 2007a); an infrared survey of the Bassett Hospital, Fort Wainwright, Alaska (Buska and Claffey 2006); and a series of infrared facility surveys from South Pole, Antarctica (Phetteplace, 2007b, 2007c, 2007d, 2007e, 2007f). However, all of these surveys used two-dimensional infrared imagery, did not attempt to georeference/switch the data together, and assessed the building envelope only through individual images. This work is the first to build a 3-D model of a building's thermal signature as a holistic view for identifying thermal deficiencies and potential construction and mitigation activities.

Independent surveys using TIR or lidar sensors have now become commonplace in assessing building envelopes. Merging these datasets postcollection is both labor intensive and complicated whereas this effort allows for the coincident collection of these data. The resulting 3-D model depicts building components at subcentimeter resolution with a thermal signature for each individual lidar point, which may then be used to accurately identify locations of heat loss contributing to energy inefficiencies. In addition, the lidar dataset has reflectance values tied to each measured surface point, corresponding to both material properties (wood, aluminum, concrete, etc.) and viewing geometry. Because the reflected light of the transmitted laser pulse varies with different building materials, a comparison between the reflectance and thermal values can help to identify building materials that are more or less energy efficient. Furthermore, by merging the 3-D thermal models of the buildings with as-built engineering drawings or computer-aided design (CAD) models of the scanned buildings, it may be possible to accurately assess the engineering approaches (e.g., construction effort and costs) for mitigating areas of significant energy loss.

1.2 Objectives

As per the Palmer Station Master Plan, USAP is assessing the infrastructure for modernization to allow the station to be a viable platform for Antarctic research for the next 35 to 50 years. In general, the master plan hopes to result in a more operationally and energy-efficient campus with predictable operational costs; reduced energy consumption for facilities and operational support; a reliable, safe, and healthy working environment for USAP personnel and visitors; and the flexibility to adapt to the changing needs of the USAP. The National Science Foundation identified three focus buildings for this project: Biolab, GWR (Garage-Warehouse-Recreation), and Terralab (Figure 1). By assessing existing building infrastructure through scanning and sensing technologies deployed during this project, USAP, NSF, and their contractors can more appropriately review their master plans.

Figure 1. Site layout for Palmer Station, Antarctica, with the three surveyed buildings (Biolab, Garage-Warehouse-Recreation, and Terralab) identified. Photo provided by the National Science Foundation.



1.3 Approach

This effort accomplishes the objectives through the following tasks:

- Deploy the lidar/TIR system to Palmer Station, Antarctica, to collect thermal and spatial measurements of the exterior of the building infrastructure.
- Tie lidar point cloud with thermal temperatures to a global coordinate system (Universal Transverse Mercator coordinate system—Zone 20 South, WGS-84 horizontal and vertical datum) using Global Navigation Satellite System (GNSS) real-time kinematic (RTK) equipment.
- Collect interior and exterior environmental conditions by using existing measurement infrastructure (permanent weather stations and interior temperature sensors) alongside temporarily deployed temperature sensors.
- Use a handheld electro-optical camera (Nikon D800) to collect standard imagery for both reference and documentation of identified areas of thermal deficiencies.

- Process all collected data, combining the lidar, TIR, and GNSS measurements to produce a 3-D thermal model (LAZ file format) of the building infrastructure.
- Analyze resulting data to identify building envelope anomalies, deficiencies, and infrastructure concerns.
- Provide resulting data to be used decision aids toward suggesting courses of action to mitigate any identified issues and to confirm the effectiveness of current building materials and design techniques.

1.4 Instrumentation platform: lidar/TIR system

A combined lidar/TIR camera system developed by CRREL was used to complete the primary data collection. This system includes the TIR sensor hard mounted to the lidar scanner in a portable package capable of being transported and operated by a single user (Figure 2). Through precise machining of the camera mount and a camera calibration procedure, the individual temperature values captured by the TIR sensor can be assigned to individual points in the laser scan data. The result is a 3-D thermal model of the measured surfaces.

Figure 2. CRREL's lidar/TIR system in use on the GWR rooftop platform, October 2015. The InfraTec VarioCAM HD camera is mounted to a Riegl VZ-1000 terrestrial laser scanner.

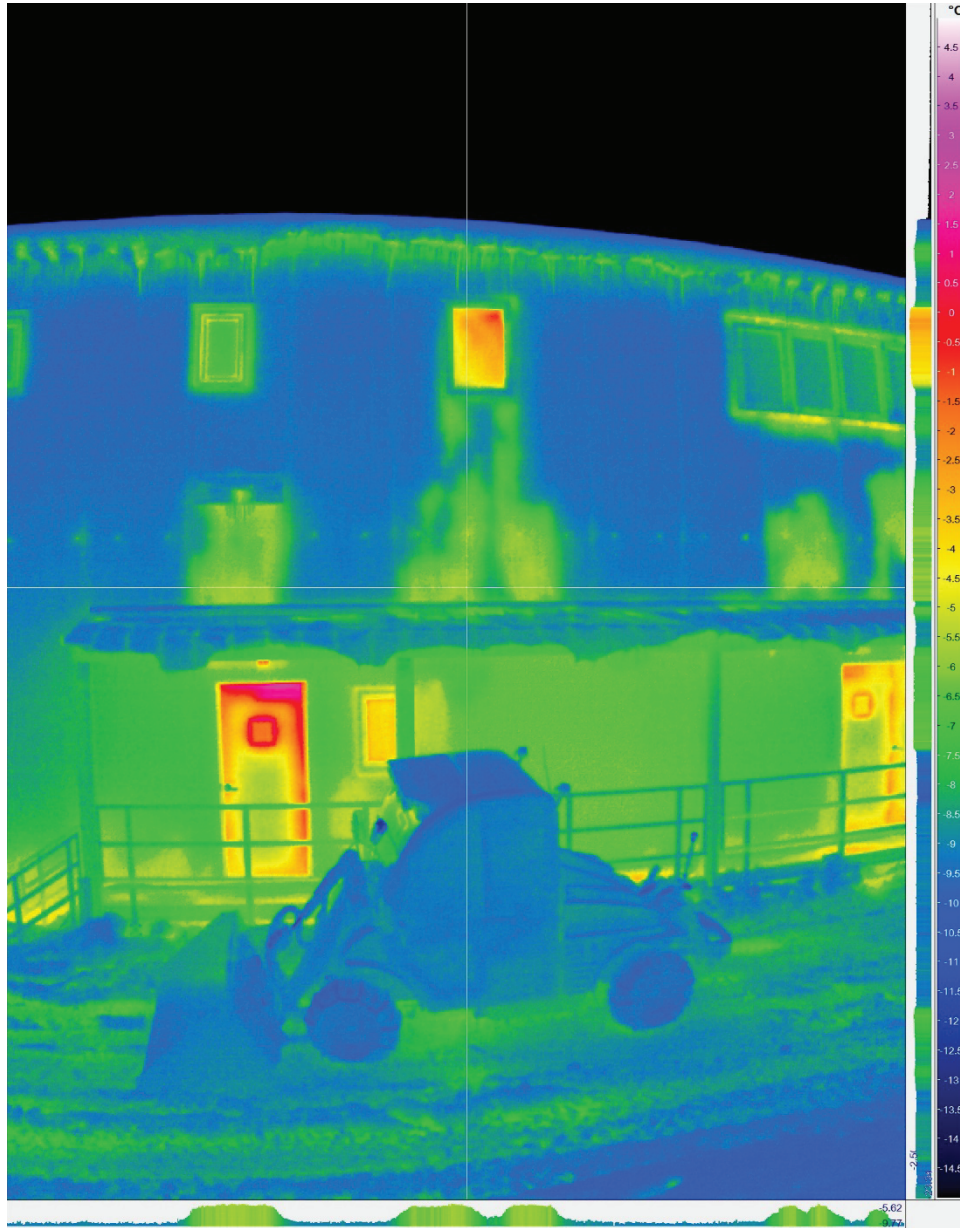


The lidar sensor is a Riegl VZ-1000 terrestrial laser scanner (TLS). This is a full-waveform sensor capable of capturing multiple returns per laser pulse. In addition to collecting lidar data, the scanner also provided the mounting platform and power for operating the TIR sensor. It uses a 1550 nm eye-safe pulsed laser to measure range and surface reflectance values over a 360° horizontal by 100° vertical field of view. The scanner is capable of measuring at ranges up to 1400 m, has a maximum pulse rate of 300 kHz, and has an accuracy/precision of 8 mm/5 mm. Additional information about the VZ-1000 terrestrial scanner may be found at <http://www.riegl.com/>.

The TIR sensor used is an InfraTec VarioCAM HD 880 sensor. The sensor uses an uncooled microbolometer focal-plane array, has a spectral range of 7.5–14 μm , and outputs a 1024 \times 768 pixel image. The sensor has a measurement range of -40°C to 1200°C , a measurement accuracy of $\pm 1.5\%$ when surface temperatures are below 0°C , and a thermal resolution better than 0.05 K at 30°C . This sensor was well within its operating range of -25°C to 50°C throughout the Palmer Station Survey with observed air temperatures ranging from -5.1°C to 24°C . A wide angle (field of view: $60^{\circ} \times 47^{\circ}$) 15 mm lens was used to best match the field of view of the laser scanner. When mounted to the laser scanner, the camera is in portrait configuration with the 60° field-of-view edge of the image aligned vertically.

The TIR sensor outputs a proprietary-format image file for each image captured. This file type, .irb, is then ingested into InfraTec's IRBIS 3 software package for both analysis and processing. The image preserves scalar radiometric values for each pixel, which can be converted or displayed as temperature values in IRBIS 3 and assigned to each pixel and exported in a variety of file formats (Figure 3).

Figure 3. Sample TIR image captured by the VarioCAM sensor. The color scale is -15°C to 5°C . Temperature profiles (vertical and horizontal) are displayed on the *bottom* and *right* of the image for the pixels intersecting with the cross hairs. The horizontal profile clearly captures insulation deficiencies below windows.



2 Data Acquisition

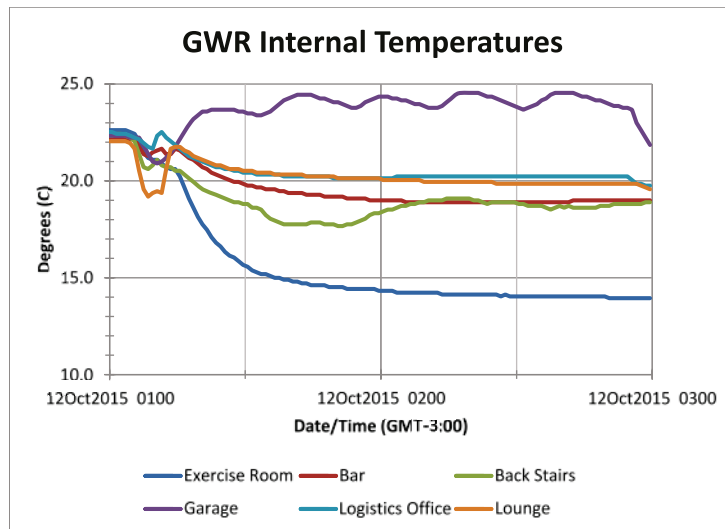
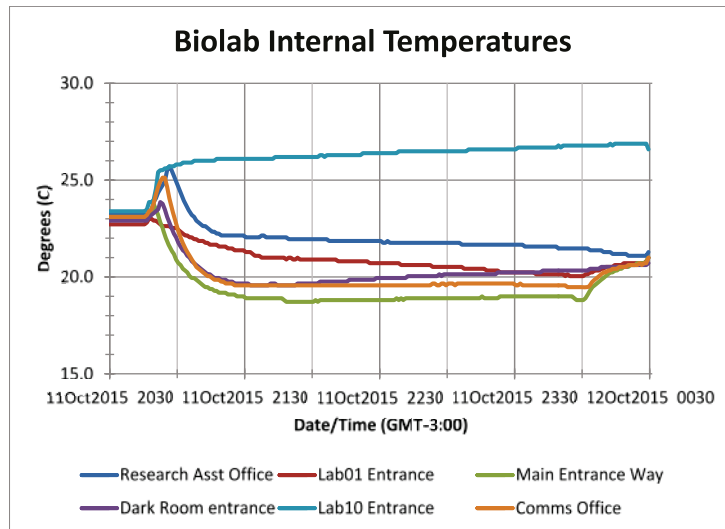
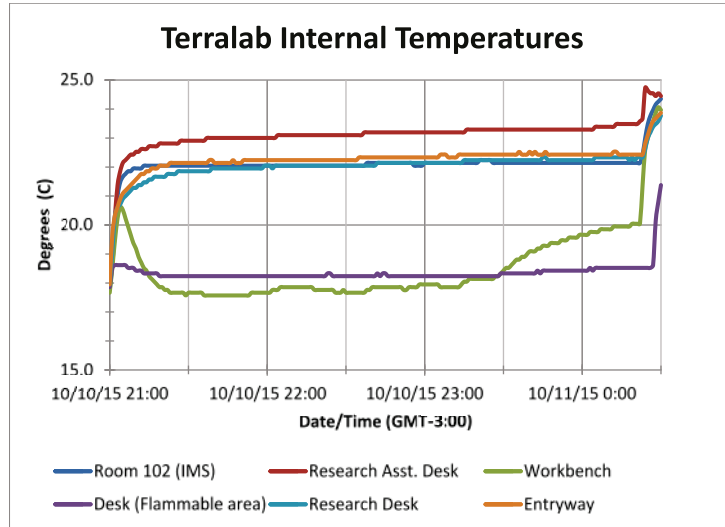
A combination of instruments, acquisition techniques, and direct logging of environmental conditions was used both to document the interior/exterior conditions and to collect the 3-D and thermal data for each focus building. These measurements aid in assessing the technique for lidar/TIR acquisitions and are a reference when discussing the results. In addition to the lidar/TIR system, the following instrumentation and techniques were used for data acquisition: interior temperature loggers, exterior climate station data, a GNSS RTK control survey, handheld TIR imagery, and handheld electro-optical imagery.

2.1 Interior temperature loggers

For coincident internal temperature measurements, a set of Onset HOBO UA-002-64 pendant loggers were used for multiple temperature logging locations within the buildings. These low-cost, small-footprint sensors have a measurement range of -20°C to 70°C , an accuracy of $\pm 0.53^{\circ}\text{C}$, and a resolution of 0.14°C at 25°C .

The data loggers were deployed in each of the assessed buildings, and the time interval for data acquisition was set to 10 seconds to monitor any internal temperature fluctuations that occurred during the external lidar and thermal scanning. For each scanning period, Figure 4 shows the set of internal building temperatures for various locations throughout each of the three buildings (Terralab, Biolab, and GWR). Temperature fluctuations at the beginning of the record are due to establishing equilibrium once data loggers were in place, and fluctuations at the end of the record are a result of the data loggers being retrieved from their stationary locations. Fluctuations throughout the record may be a result of heating systems cycling on/off, drafty conditions, or external doors opening and closing near the data loggers.

Figure 4. Internal building temperatures from various locations within each of the three buildings at the time of external lidar and thermal scanning.



2.2 Exterior climate station data

Palmer Station, Antarctica, is part of NSF's Long-Term Ecological Research (LTER) sites and therefore has collected weather data in coordination with its operations. Acquisition of weather data began in 1989. In November of 2001, an automatic weather station was installed, and the PALMOS automatic weather station data came online on 13 December 2003. In total, these data include a daily averaged weather time series from 1 April 1989 through the present (Information Manager, PAL, 2016).

Figure 5 includes the historical temperature time series processed into a daily climatology of minimum, maximum, and average temperature over the period of record (1986 to 2016). In general, for the month of October, temperatures do increase; however, the average daily temperatures are typically below freezing (approximately -2.5°C). Table 1 highlights the lidar and thermal scan times for the three Palmer Station buildings, and Figure 6 shows the historical daily temperatures along with the actual daily temperature from the climate station during deployment. For the purpose of this assessment and through a general comparison of the internal and external temperatures (Figures 4 and 5, respectively), there is a significant temperature gradient (greater than 15°C) between the indoor and outdoor temperatures, allowing for a meaningful assessment of the thermal building envelope through the external lidar and thermal scanning activities.

Figure 5. Palmer Station temperature climatology.

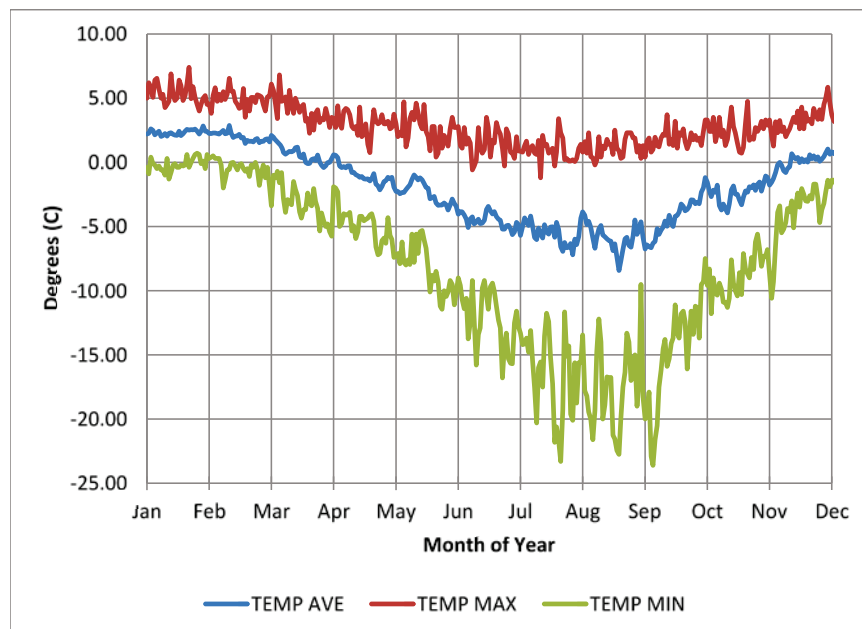
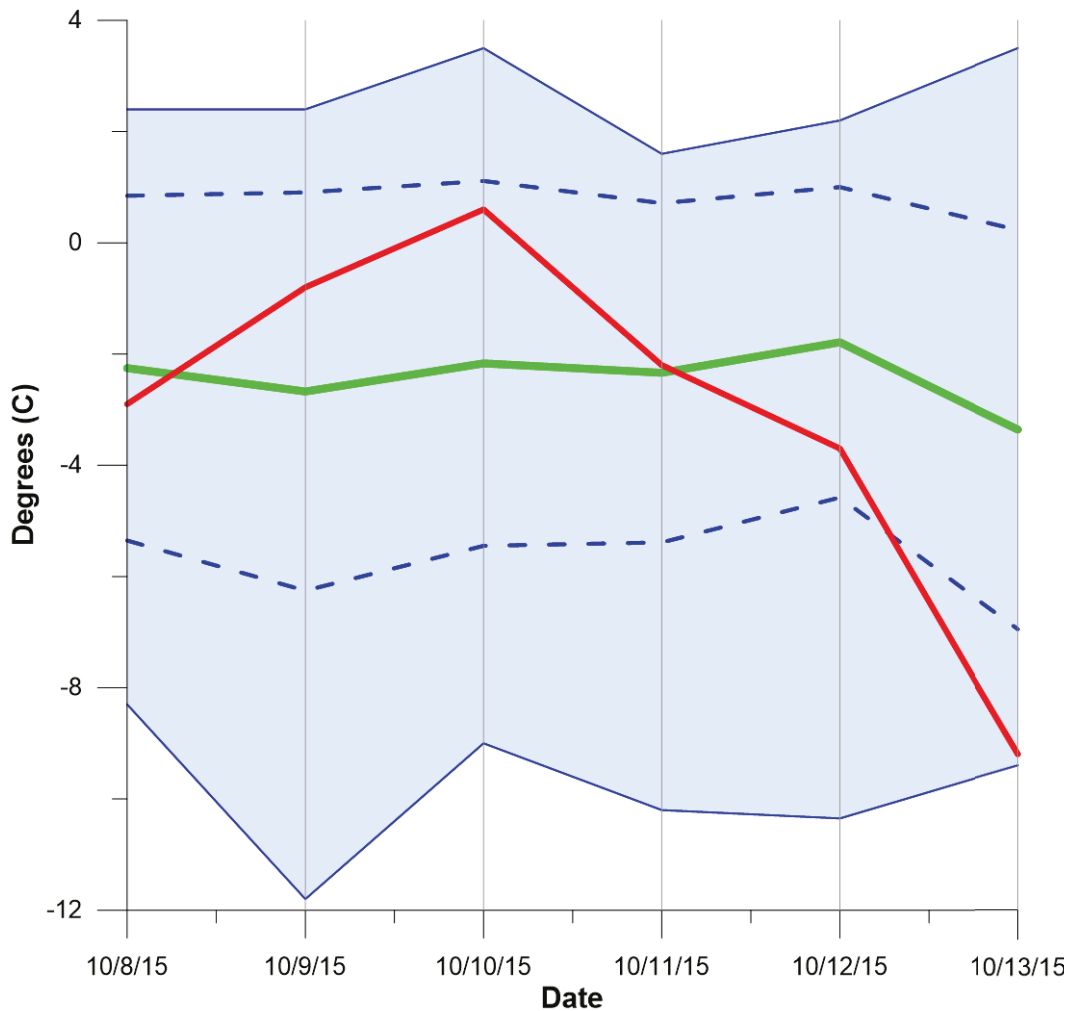


Table 1. Lidar and thermal acquisition dates/times at Palmer Station.

Building	Scan Date/Time (GMT)	Scan Date/Time (GMT-3)
Terralab	11 Oct 2015 00:00 to 11 Oct 2015 03:00	10 Oct 2015 21:00 to 11 Oct 2015 00:00
Biolab	11 Oct 2015 23:30 to 12 Oct 2015 03:00	11 Oct 2015 20:30 to 12 Oct 2015 00:00
GWR	12 Oct 2015 04:00 to 12 Oct 2015 06:00	12 Oct 2015 01:00 to 12 Oct 2015 03:00

Figure 6. For the dates of deployment, Palmer Station daily temperature (*red*) and temperature climatology (*green* = historical mean; *solid blue* = historical minimum and maximum; *dashed blue* = ± 1 standard deviation from the mean).



2.3 GNSS RTK control survey

This project required the lidar point clouds to be tied to a global coordinate system to record the orientation of the building faces and to measure the aspect of the building surfaces. This process, called georeferencing,

was completed at Palmer station by conducting an RTK survey for temporary reflectors set up within view of the laser scanner. Palmer Station runs a continuously operating reference station that broadcasts a radio signal for RTK surveys. It is only necessary to have one lidar scan with the RTK-surveyed reflectors visible to georeference the entire dataset. The “Lidar registration/georeferencing” section will discuss this further.

Two RTK surveys were conducted at Palmer Station: the first on 10 October 2015 and the second on 12 October 2015. For each RTK survey, three 10 cm reflector cylinders were set up throughout the survey area (Figure 7). These reflectors were visible from multiple scan positions. The reflector has a reflective tape face 10 cm in height \times 10 cm in diameter that is highly visible in the point cloud, allowing the precise shape and location of the cylinder to be recorded and identified. Each reflector was surveyed, and a height offset from the GNSS antenna was applied to measure the centroid of each reflector cylinder. Table 2 is a list of all recorded values from the two RTK surveys. Resulting measurements from both RTK surveys yielded an average horizontal precision of 0.005 m and vertical precision of 0.011 m.

Figure 7. Example image of a 10 cm reflector cylinder with a reflective tape face used in georeferencing lidar point clouds.



Table 2. Recorded values from the RTK surveys of the 10 cm reflector cylinders used for georeferencing the lidar point clouds.

Palmer Station 2015 LiDAR/TIR Ground Control Survey

Measurement	2015/10/10			2015/10/12		
	TP001	TP002	TP003	TP001	TP002	TP003
Latitude	64° 46' 27.40092" S	64° 46' 28.37823" S	64° 46' 27.25686" S	64° 46' 28.33009" S	64° 46' 27.32508" S	64° 46' 27.86385" S
Longitude	64° 03' 11.51934" W	64° 03' 12.07505" W	64° 03' 06.35987" W	64° 03' 11.92184" W	64° 03' 11.55693" W	64° 03' 10.48982" W
Height (WGS84)	24.703	23.770	31.255	24.201	24.759	25.695
Horizontal Precision (m)	0.005	0.006	0.005	0.004	0.007	0.004
Vertical Precision (m)	0.010	0.011	0.010	0.010	0.017	0.010
Satellite (min)	9	9	9	9	10	9
RDOP (max)	2.1	2.3	1.8	1.5	2.8	3.1
HDOP (max)	0.9	1.1	0.8	0.6	1.1	1.2
VDOP (max)	1.8	2.0	1.6	1.3	2.6	2.9
Positions Used	16	16	16	16	16	16
Start Local Date	2015/10/10	2015/10/10	2015/10/10	2015/10/12	2015/10/12	2015/10/12
Start Local Time	04:29:52	04:28:21	04:32:23	07:02:20	07:03:52	07:04:53
Stop Local Time	04:30:07	04:28:36	04:32:38	07:02:35	07:04:07	07:05:08
RMS	8.9	12.1	11.0	10.4	14.4	16.7
UTM Zone	20S	20S	20S	20S	20S	20S
Easting (m)	449917.700	449910.880	449985.811	449912.900	449917.185	449931.536
Northing (m)	2816284.882	2816254.562	2816290.472	2816256.044	2816287.214	2816270.845
Corrected Height (WGS84) (m)	24.6218	23.6888	31.1738	24.1198	24.6778	25.6138

2.4 TIR handheld imagery

In addition to the lidar/TIR system, a FLIR SC640 handheld TIR camera was used for the collection of areas either not covered by the lidar/TIR system's field of view or areas that demanded higher detail. The SC640 has similar technical specifications to the VarioCAM HD 880 sensor, with the following main differences: spectral range of 7.5–13 μm , 640 \times 480 pixel image, measurement range of -40°C to 1500°C , measurement accuracy of $\pm 2^{\circ}\text{C}$ or $\pm 2\%$ of the reading, and operating temperature range of -15°C to 50°C . Like the VarioCAM sensor, the SC640 fell within its operating temperature range while at Palmer Station. Figure 8 is an image of the SC640 in use at Palmer Station.

Figure 8. CRREL's Dr. Elias Deeb operating the FLIR SC640 during daytime for comparison to nighttime image collections.



2.5 Electro-optical (EO) imagery

Handheld electro-optical imagery, using a Nikon D800 camera, was collected for all exterior building surfaces to confirm results observed with the integrated lidar/thermal instrumentation, to assist in the identification of complicated building geometries, and to further explore areas not conducive for the larger automated scanner. The location of each image capture is documented in the “Palmer Station EO Camera Survey: October 10, 2015” map found in Appendix A. The corresponding images are named with the following naming convention: *Palmer_EO_Position_(XXx).JPG*. The images are archived and are available upon request.

2.6 Lidar/TIR system acquisition

Lidar scans and TIR imagery were acquired from multiple system setups throughout Palmer Station. The combined lidar/TIR system is composed of the VZ-1000 laser scanner with the VarioCAM HD sensor mounted externally to the top of the scanner. An external battery pack supplied power to the scanner, which in turn provided power to the camera. Both sensors were controlled via Ethernet cable using a ruggedized PC (Figure 9). The system was attached to a survey tripod, which was set up temporarily at each scan position. For scan positions on deep, unconsolidated snowpack, sections of snow were cleared; and each tripod foot was driven into the snow manually. It is important to be aware of potential settlement of the

tripod during acquisition so that the geositional accuracy of the collected points is not compromised. Settlement during acquisition may cause positional inaccuracies of the collected points the farther away they are from the scanner position. For this case, the on-scanner inclination sensor did not indicate significant settlement, the scan time was relatively short (on the order of minutes), and the scanner position was close to the objects being scanned. These all contribute to a low (to negligible) error budget for any potential settlement during scanning.

Figure 9. CRREL's Adam LeWinter collecting data at Palmer Station using the lidar/TIR System.



The CRREL Lidar Group developed the lidar/TIR system in cooperation with Riegl Laser Measurement Systems (www.riegl.com). As a result, the system is a custom solution to capturing and coregistering thermal values to a 3-D point cloud. The solution is a semiautomated process that involves the collection of traditional terrestrial laser scan data and manual triggering and capture of the TIR sensor at each scan position. A detailed step-by-step acquisition procedure is included in Appendix B. For each scan position, a high-resolution lidar scan was captured with the following scanning parameters: 100° vertical \times 360° horizontal field of view, 0.03° angular increment (both vertically and horizontally), and a 300 kHz pulse repetition rate. These scan parameters resulted in roughly 13- to 20-million points/scan, with centimeter- to subcentimeter-scale point spacing on the focus-building surfaces. At the conclusion of each lidar scan, TIR images were captured with a 40° horizontal overlap to ensure total coverage of the scan area.

Both lidar and TIR are considered line-of-sight sensors in that objects within the line of sight are imaged, causing shadows (or missing data) behind these objects; therefore, it was necessary to collect multiple scan positions surrounding the focus infrastructure to best capture all exterior surfaces. However, some surfaces of the focus infrastructure were obstructed from all views due to snowdrifts in contact with the buildings, supporting structures and vehicles located alongside building walls, and an inability to access suitable scan positions. All efforts were made to minimize these data “gaps.”

Five coincident lidar/TIR surveys were conducted between 9 and 12 October 2015 during varying weather conditions. Appendix A provides individual survey maps indicating location and number of scan positions, reflector positions, and electro-optical imagery capture positions. Appendix C provides a detailed log of each survey, including acquisition time, atmospheric observations (air temperature, relative humidity, barometric pressure, and wind speed), and scanning notes. All successful exterior scans were conducted at night, without direct sunlight and without precipitation, to limit the influence of ambient light, solar radiation, and thermal homogeneity on the TIR imagery.

While the lidar scanner, which uses online-waveform processing to capture multiple returns per pulse, is capable of successfully capturing focus surfaces through snowfall, the TIR sensor does not perform well. Figure 10 provides a comparison between TIR images captured during both atmospheric conditions. Therefore, it was necessary to wait for optimal weather conditions devoid of snowfall and blowing snow. The first two surveys, conducted on 9 and 10 October 2015, were terminated early due to heavy blowing snow. A full survey of the Biolab was conducted on 10 October 2015 but was deemed suboptimal as it was conducted in full daylight. Optimal weather conditions occurred on 11 to 12 October 2015 where all exterior scans for Biolab and GWR (11 October 2015) and Terralab (12 October 2015) were collected under little to no precipitation during the night.

Figure 10. Comparison of lidar data collected without snow precipitation (*top*) and with significant falling and blowing snow, highlighted by reflectance, in *red* (*bottom*). While the lidar system is capable of measuring the building surface through snowfall, the building surface resolution is reduced, and the thermal values are skewed.



3 Data Processing

3.1 Lidar registration/georeferencing

With the GNSS RTK survey and scanning of the 10 cm reflector cylinders arranged throughout the Palmer Station site, all point clouds were tied to a global coordinate system. Single point measurements in the point cloud have X (longitude), Y (latitude), and Z (elevation) values associated. Triangulation was used to tie observed GNSS coordinates to measured reflector positions. For both surveys that incorporated RTK-measured reflectors (9–10 October and 12 October surveys), the measured coordinates of the reflectors were entered into the acquisition and processing software package (RiSCAN Pro, www.riegl.com) for the centers of the reflector cylinders. At least one scan position per survey was positioned so that all three reflectors were within the scanner field of view. Through triangulation, this scan was used as the baseline georeferenced scan. See Appendix A for map layouts of scanner and reflector positions.

Subsequent scans around the buildings were tied to the baseline georeferenced scan through two processes: coarse registration and Multi Station Adjustment (MSA). Coarse registration involves finding a minimum of four common points between overlapping scans to roughly align the point clouds together. While coarse registration provides a start to the registration/georeferencing process, it does not provide a precise fit of the point clouds to each other, with typical positional errors on the centimeter to meter scale. To better align multiple scans and to reduce error, MSA identifies and uses corresponding planar surface areas from overlapping point clouds. MSA involves the calculation of planar surfaces given user input of specific variables, including the minimum number of points required to define a plane and the minimum/maximum search area to define a plane. The calculated planes from different scans are then aligned, resulting in a typical positional error between multiple point clouds in the subcentimeter scale.

Beginning with the baseline georeferenced scan, neighboring scans with significant overlapping points were coarse registered and then run through the MSA process to finalize all of the scan positions. At this point, the point clouds are all registered and georeferenced and can be viewed as a single data collection product.

3.2 Temperature value registration

Because a separate sensor collected the thermal images, the temperature values within the images must be mapped and assigned to the individual points within the point cloud. Both a camera calibration and a camera-mount calibration matrix were created within RiSCAN Pro, mapping the camera/lens field of view to the field of view of the laser scanner. This results in the ability to assign a temperature value to an individual point, as measured by the thermal camera, based on the scan angle (vertical and horizontal) of the point measurement. CRREL has developed custom, open-source code to complete this process in which the temperature value (°C) is assigned to individual points within the LAS file format. For further details on this process, see Appendix B: CRREL Lidar/TIR System Data Acquisition Procedure.

4 Results and Discussion

4.1 Biolab

There were significant areas of temperature anomalies observed on the exterior of the Biolab. The roofline soffits, which had varying levels of gap-filling insulation material with large sections missing, displayed significant heat loss (Figure 11). Additionally, apparent degradation of insulation directly below windows indicates damage caused by leaking or insufficient insulation. This was observed in both the Biolab and GWR buildings. Unlike GWR, all windows in the Biolab appear to be of the same make and style throughout the building. As expected, doorways also displayed heat loss. Sections along the exterior surfaces adjacent to the ceiling/floor interfaces between floor levels displayed slight temperature differences, particularly along the southeast wall. Figures 12–15 provide a sample of observed deficiencies. These images are taken of the point cloud colored by temperature, with color scale bars provided.

Figure 11. Detail of damaged or unseated insulation along southwest roofline soffits on the Biolab. Multiple areas were completely devoid of this insulation material.



Figure 12. Southwest face of Biolab. Significant venting of heat was observed at the ground-level doorway, along the lower connection of the cafeteria deck, at the cafeteria deck exit, and along the roofline soffit. In addition, degradation of insulation is evident below the upper-level windows. Temperature scale: -15°C to 5°C .

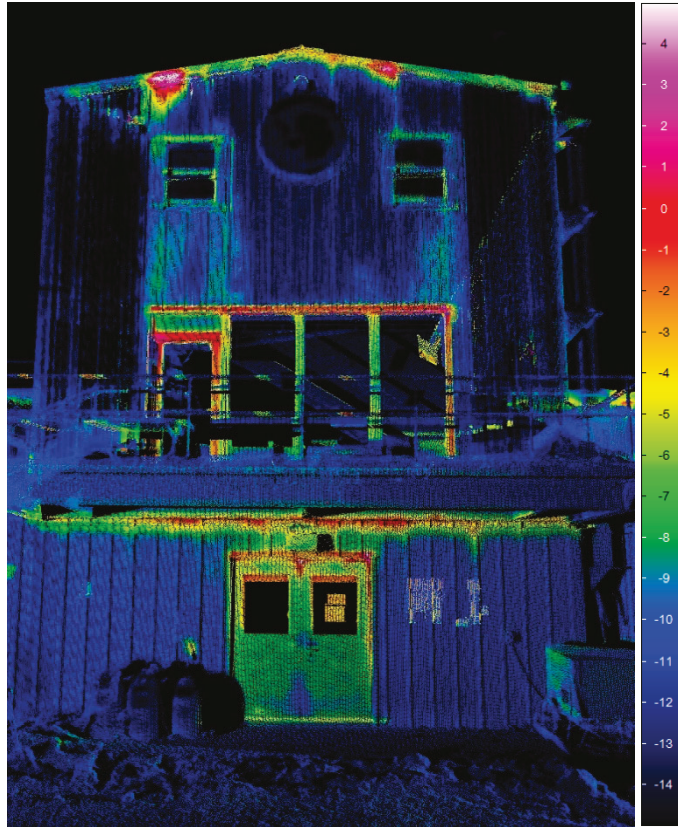


Figure 13. Ground-level entrance and vestibule on the south-southwest section of Biolab. Higher surface temperatures were measured at the entrance and within the vestibule. The second- and third-level soffits show heat loss. Some heat loss was observed along exterior metal sheeting overlaps. Temperature scale: -15°C to 5°C .

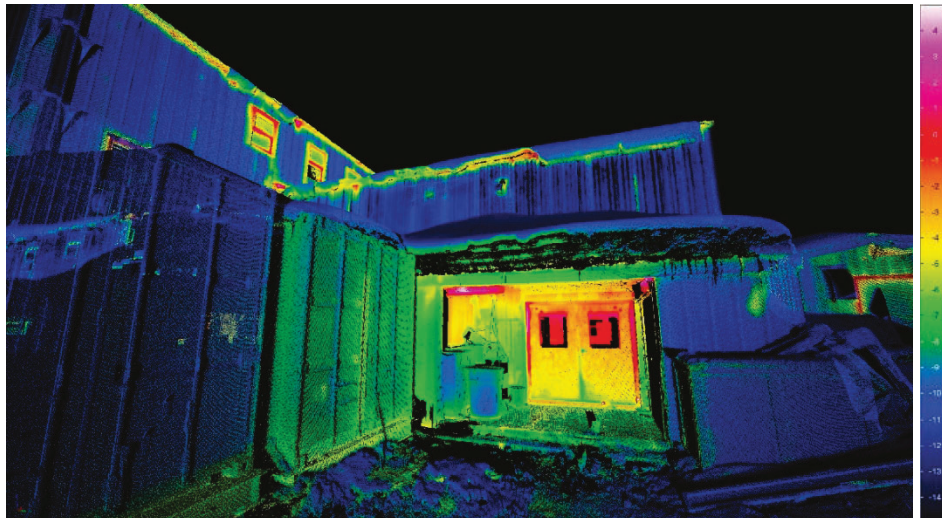
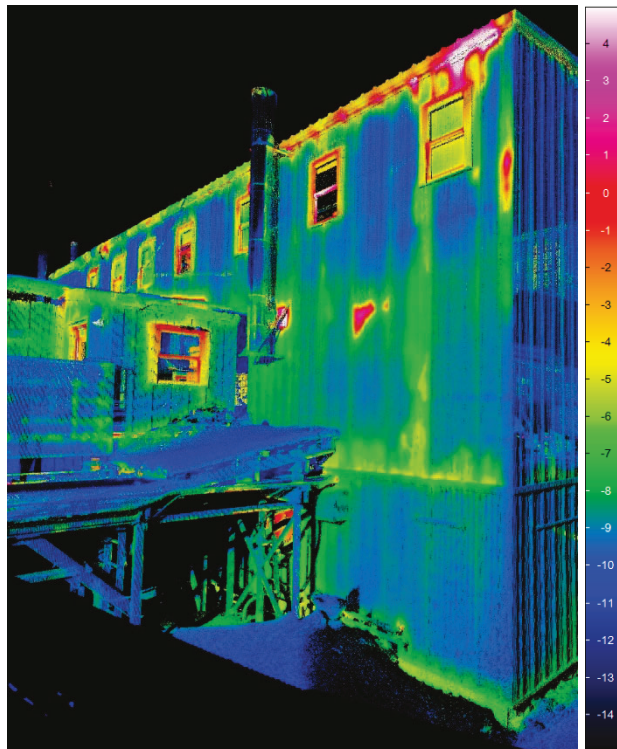


Figure 14. Southeast face of Biolab, including the walkway and entrance into the kitchen/cafeteria. Significant heat loss was observed along the top soffit with the highest temperature values measured on far right side of the image. Windows display varying levels of heat loss. There is degradation of insulation below the upper windows, possibly from water leaking. The ceiling level of the ground level/floor of second level has heat loss along the exterior. Temperature scale: -15°C to 5°C .



Figure 15. Southeast face of Biolab. The far right of the roofline shows significant heat loss along the roofline soffit. There is degradation of insulation below upper windows, possibly due to water leaking. The ceiling of the ground level and floor of the second level has heat loss along the exterior. A hot spot is visible to the right of the kitchen exhaust vent. Temperature scale: -15°C to 5°C .



4.2 GWR

While there were sections of expected heat loss on the exterior of the GWR building (e.g., generator exhaust, garage doors, and doorways), significant heat loss was measured below many of the windows (Figures 16–19). Specifically, two window types were present: smaller black-trim windows in recessed frames and larger white-trim windows mounted essentially flush with the exterior metal panels. While the black-trim windows displayed little to no heat loss below their frames, all white-trim windows had large temperature anomalies. This appears visually in the temperature-colored point cloud as a “leak” below each window. This is likely due to either leaking then subsequent damage to insulation or insufficient seals between the window frame and exterior panels/insulation. Figure 20 also shows an example scan of the interior of the garage bay in the GWR building where an increasing temperature gradient is evident from the floor to the ceiling as well as areas of cold ingress and heat loss around the garage door and entry doorway.

Conversely, the seams between individual metal panels facing the exterior displayed very little heat loss, indicating quality construction and seal. This is apparent by the uniform surface temperatures along the exterior, not including the above-mentioned window leaks.

Figure 16. South face of GWR. There is significant degradation below white-trim windows (see Fig. 17 for the electro-optical image). Smaller, black-trim windows display no leaking of heat below the frames, indicating a better seal. Heat loss is observed along the roofline soffit, though not as large of a temperature difference compared to observations of the Biolab soffits. Lower portions of the building were obstructed by heavy equipment parked by the building, a necessity for charging and heating purposes. Temperature scale: -15°C to 5°C .

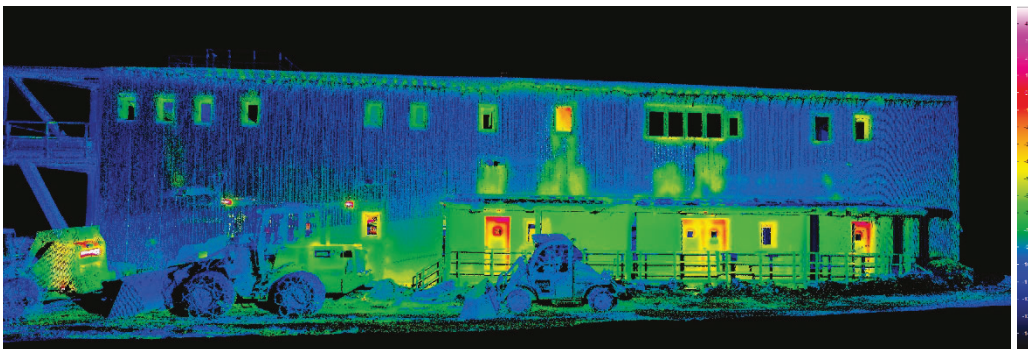


Figure 17. Detail images from the south face of GWR. The *top* image, captured with the handheld DSLR camera, demonstrates the two main types of windows in use in GWR: black-trim and white-trim. The white-trim windows clearly show significant heat loss below while no temperature differences were measured below the smaller black-trim windows. Temperature scale for the bottom image: -15°C to 5°C .



Figure 18. East face of GWR, displaying significant heat loss and insulation damage below white-trim windows. The damage to insulation continues from the top-floor windows fully down to ground level. A patched panel to the right of the windows also displays heat loss below. No significant heat loss was measured along the roofline or exterior panel seams. Temperature scale for the bottom image: -15°C to 5°C .

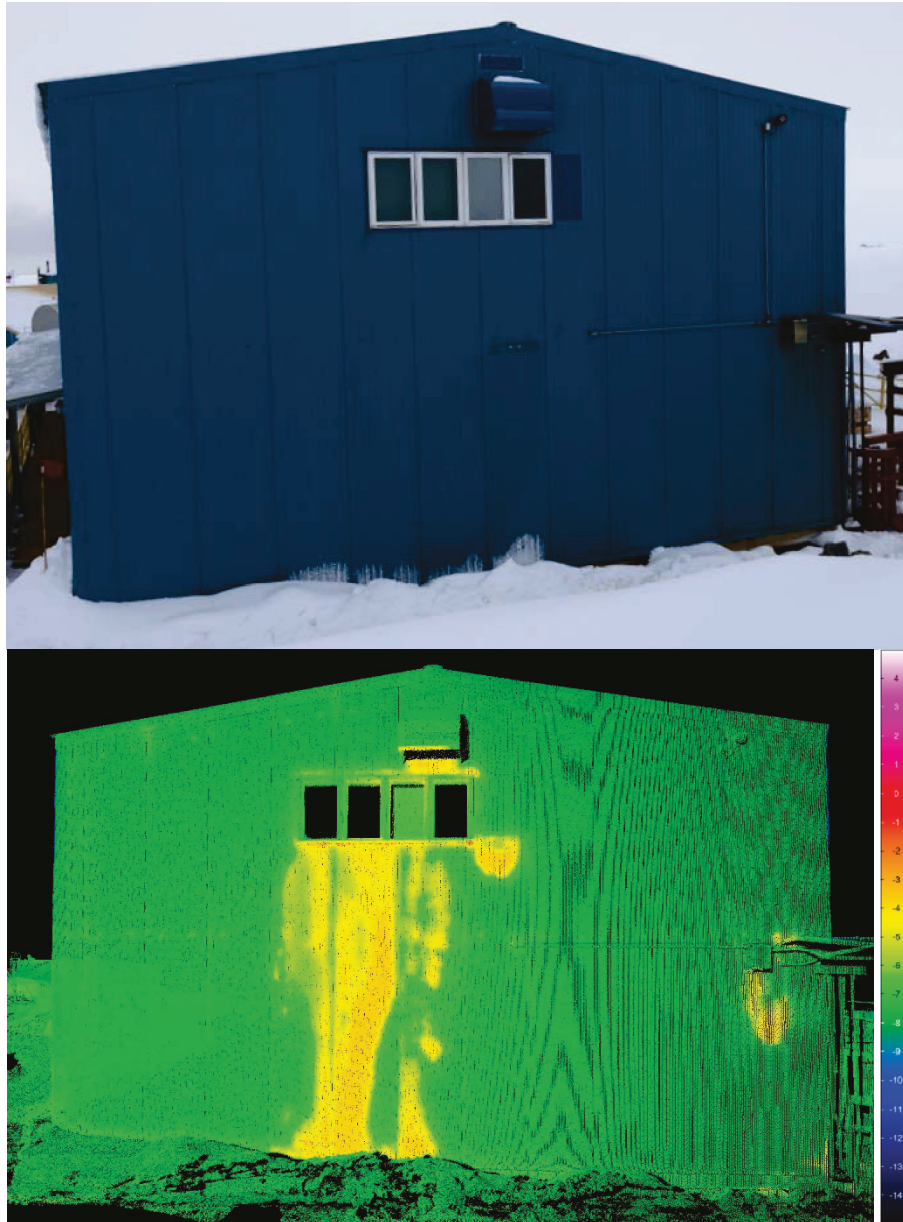


Figure 19. Significant heat loss below all windows along the GWR north side. All windows are white-trim style. Temperature scale: -15°C to 5°C .

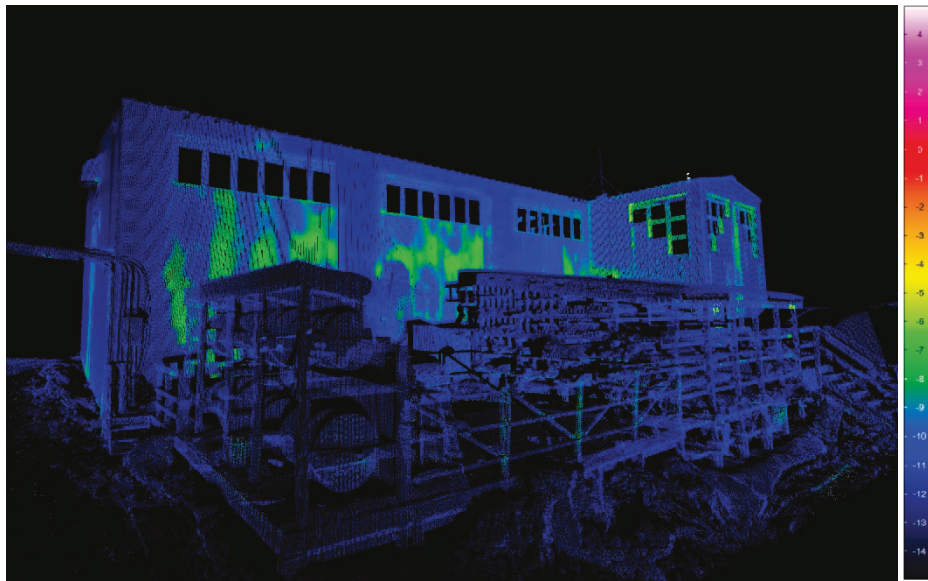
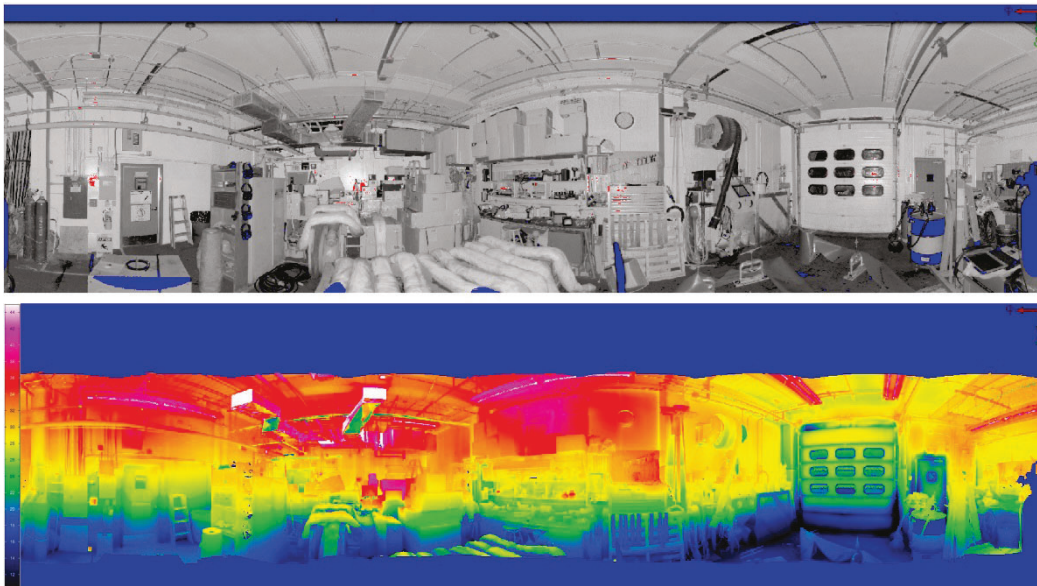


Figure 20. Interior scan of the garage bay in GWR. The *top* image is a two-dimensional view of the point cloud colored by surface reflectance in the lidar laser wavelength (dark-to-light equals low-to-high surface reflectance). The bottom image is the same view colored by temperature. An even gradient from the floor up in temperature is visible along with areas of cold ingress and heat loss around the garage door and entry doorway. Temperature scale for the bottom image: 10°C to 45°C .



4.3 Terralab

Terralab, in comparison to both GWR and Biolab, had a significantly lower temperature differential between its exterior surfaces and therefore a more uniform temperature gradient when observing the thermal envelope 3-D

model. No significant heat loss was observed along wall seams, exterior panels, windows, or soffits or on the exposed bottom of the building. The most significant temperature gradients were observed on the entryway doors and a vent on the northwest corner of the building (both indicated below in Figure 21). While there are slight temperature differences along the exterior panel seams (light colored grid), this does not seem to be attributed to heat loss but due to heat absorption of differing colors of materials (Figures 21–22). Again, an example of an interior scan of the Terralab (Figure 23) shows interesting features of thermal bridging between studs and rafters and, in contrast to the Biolab and GWR buildings, minimal cool air ingress along all of the windows, indicating better insulating performance.

Figure 21. Visible image (*top*) and lidar/TIR image (*bottom*) of Terralab. Small temperature gradients along the exterior panel seams are visible. The most significant heat loss occurs at the entryway doors and a vent halfway up the image foreground support post. Overall, this building appears sufficiently insulated. Temperature scale for the bottom image: -10°C to 5°C .

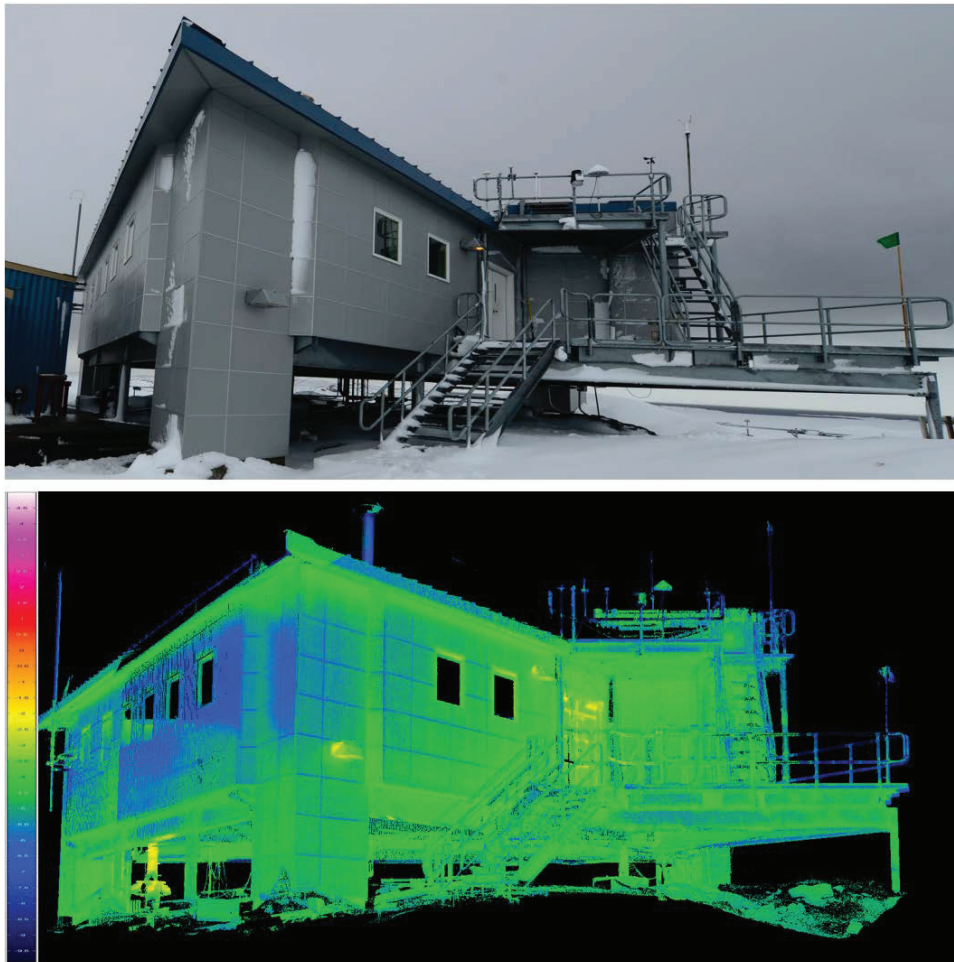
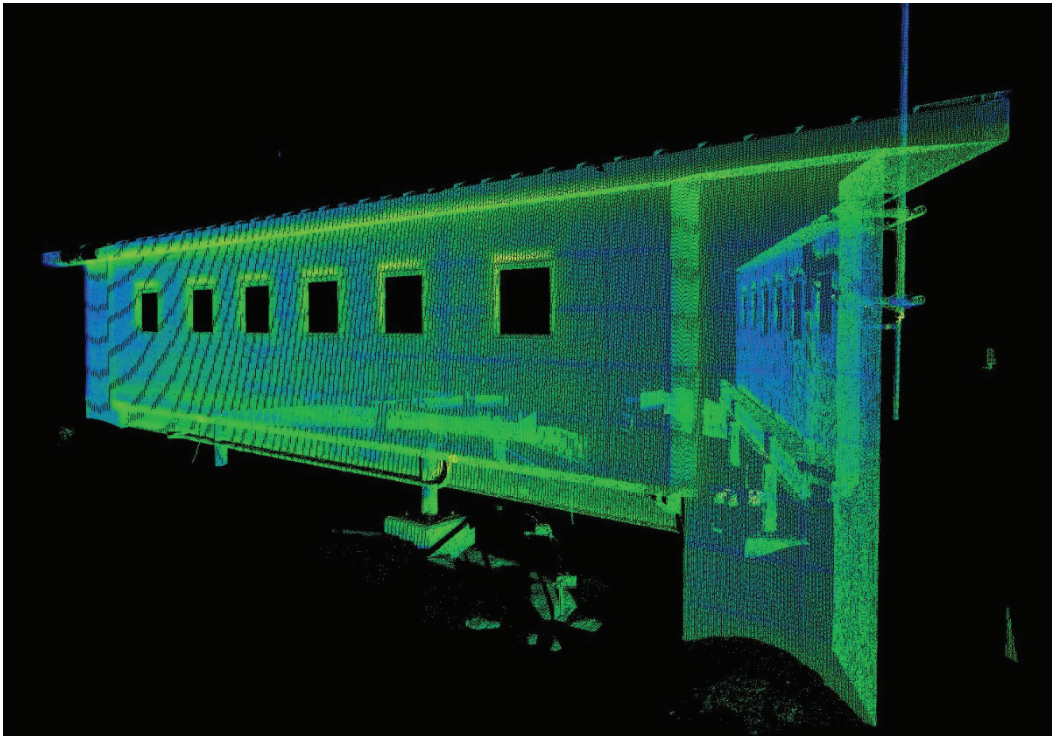
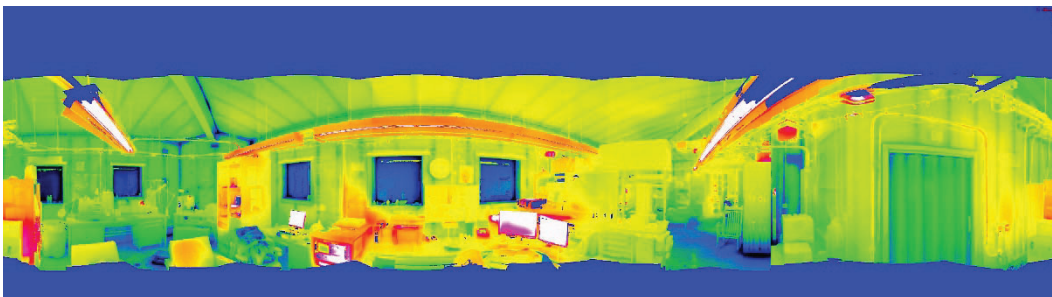


Figure 22. Temperature-colored point cloud view of the southeast side of Terralab.
Temperature scale: -10°C to 5°C (same temperature scale as Fig. 21).



For the interior of Terralab, a temperature gradient was measured from low to high along with cool air ingress and heat loss along wall seams and corners. Studs and rafters are visible within the thermal data. Of note is the minimal cool air ingress surrounding all of the windows, indicating that these windows are performing well in the conditions.

Figure 23. Panorama of the interior of Terralab's south room. Slight cool air ingress is visible along the wall-ceiling interface. Studs and rafters are visible through the drywall. Of note is the minimal cool air ingress along all of the windows, indicating that they are performing very well. Temperature scale: 17°C to 30°C .



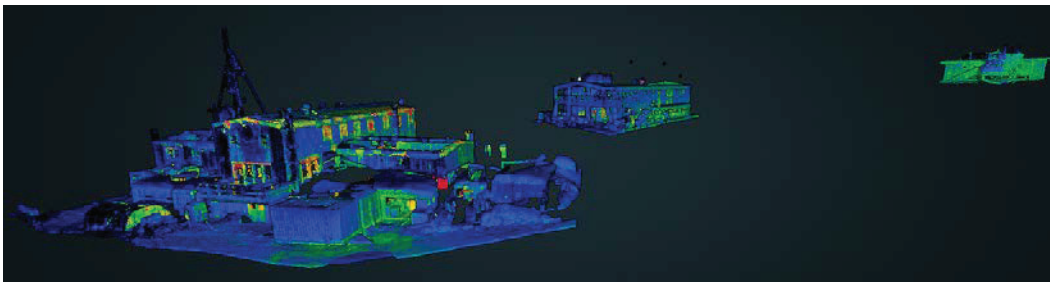
5 Conclusions

During a short time on station (approximately 9–12 October 2015), a combined lidar/TIR Camera system was deployed to Palmer Station, Antarctica, where the three major building infrastructure features were scanned to help identify and confirm construction deficiencies, to determine potential remediation steps, and to inform the Palmer Station Master Plan. Initial results and scanned models were presented within a month of deployment and resulted in a wealth of data and knowledge regarding the condition of the existing building infrastructure at Palmer Station.

In general, common thermal deficiencies appeared around windows and doorways (expected), along roofline soffits, within potential gaps of insulation, and near areas with possible degradation of insulation due to water damage. These were observed through the lidar/thermal datasets presented for both the Biolab and GWR buildings. In contrast, the more modern (in design and construction) Terralab did not exhibit large temperature gradients across exterior surfaces, having a more uniform thermal signature.

Through this effort, a web-based portal for viewing the 3-D thermal models was prototyped, tested, and provided to the National Science Foundation (Figure 24). Please contact the authors for access to the web-based portal.

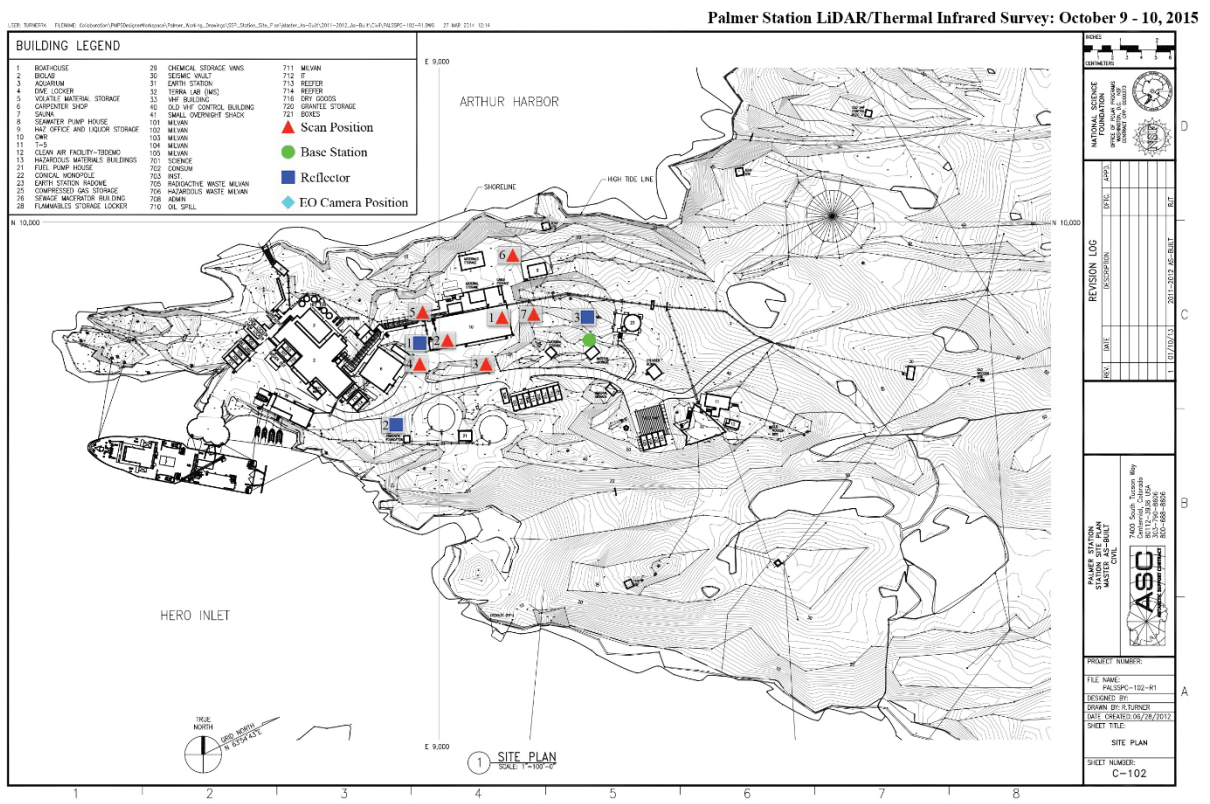
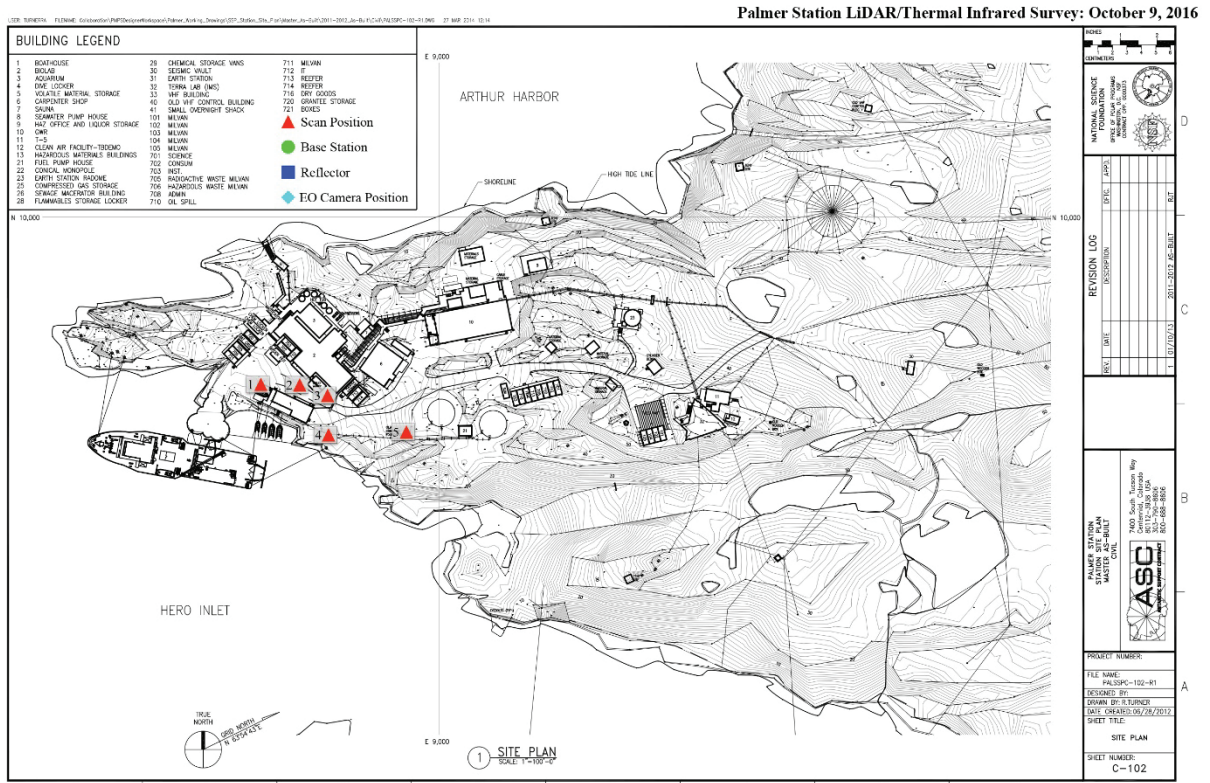
Figure 24. Screen shot of the lidar/TIR survey data for the three major buildings at Palmer Station, Antarctica, in the web-based portal.



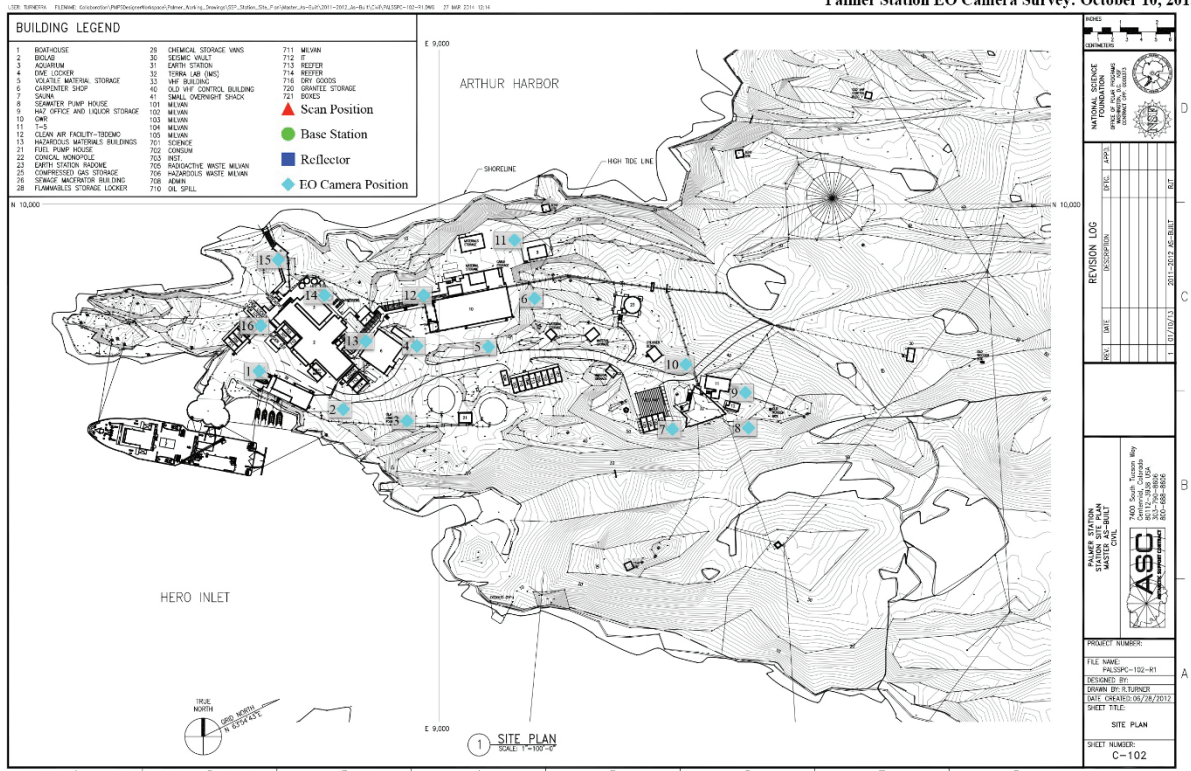
References

- Barna, L. A., K. J. Claffey, J. S. Buska, and J. L. Mercer. 2011. *Engineering Assessment of Big House at Summit Station, Greenland*. ERDC/CRREL TR-11-10. Hanover, NH: U.S. Army Engineer Research and Development Center.
- Buska, J., and K. Claffey. 2006. *An Infrared Survey of the New Bassett Hospital, Fort Wainwright, Alaska*. ERDC/CRREL LR-06-7. Hanover, NH: U.S. Army Engineer Research and Development Center.
- Information Manager, PAL. 2016. *Daily Averaged Weather Timeseries (Air Temperature, Pressure, Wind Speed, Wind Direction, Precipitation, Sky Cover) at Palmer Station, Antarctica Combining Manual Observations (1989–Dec 12, 2003) and PALMOS Automatic Weather Station Measurements (Dec 13, 2003–present)*. Palmer Station, Antarctica: Long-Term Ecological Research Network. <http://dx.doi.org/10.6073/pasta/50627a6eb69afce74859b8349d9f8dc4>.
- Phetteplace, G. 2007a. *Infrared Survey of the Elevation Station, 2006–2007 Season, South Pole, Antarctica*. ERDC/CRREL LR-07-09. Hanover, NH: U.S. Army Engineer Research and Development Center.
- . 2007b. *Infrared Thermography of the Building Envelope of the Ice Cube Laboratory, South Pole, Antarctica*. ERDC/CRREL LR-07-04. Hanover, NH: U.S. Army Engineer Research and Development Center.
- . 2007c. *Infrared Thermography of the Building Envelope of the Martin A. Pomerantz Observatory, South Pole, Antarctica*. ERDC/CRREL LR-07-05. Hanover, NH: U.S. Army Engineer Research and Development Center.
- . 2007d. *Infrared Thermography of the Building Envelope of the Dark Sector Laboratory, South Pole, Antarctica*. ERDC/CRREL LR-07-06. Hanover, NH: U.S. Army Engineer Research and Development Center.
- . 2007e. *Infrared Thermography of the Building Envelope of the Atmospheric Research Observatory, South Pole, Antarctica*. ERDC/CRREL LR-07-07. Hanover, NH: U.S. Army Engineer Research and Development Center.
- . 2007f. *Infrared Thermography of the Building Envelope of the New Cryogen Facility, South Pole, Antarctica*. ERDC/CRREL LR-07-08. Hanover, NH: U.S. Army Engineer Research and Development Center.
- U.S. Antarctic Program Blue Ribbon Panel. 2012. *More and Better Science in Antarctica through Increased Logistical Effectiveness*. Washington, DC: National Science Foundation, U.S. Antarctic Program. https://www.nsf.gov/geo/opp/usap_special_review/usap_brp/rpt/antarctica_07232012.pdf.

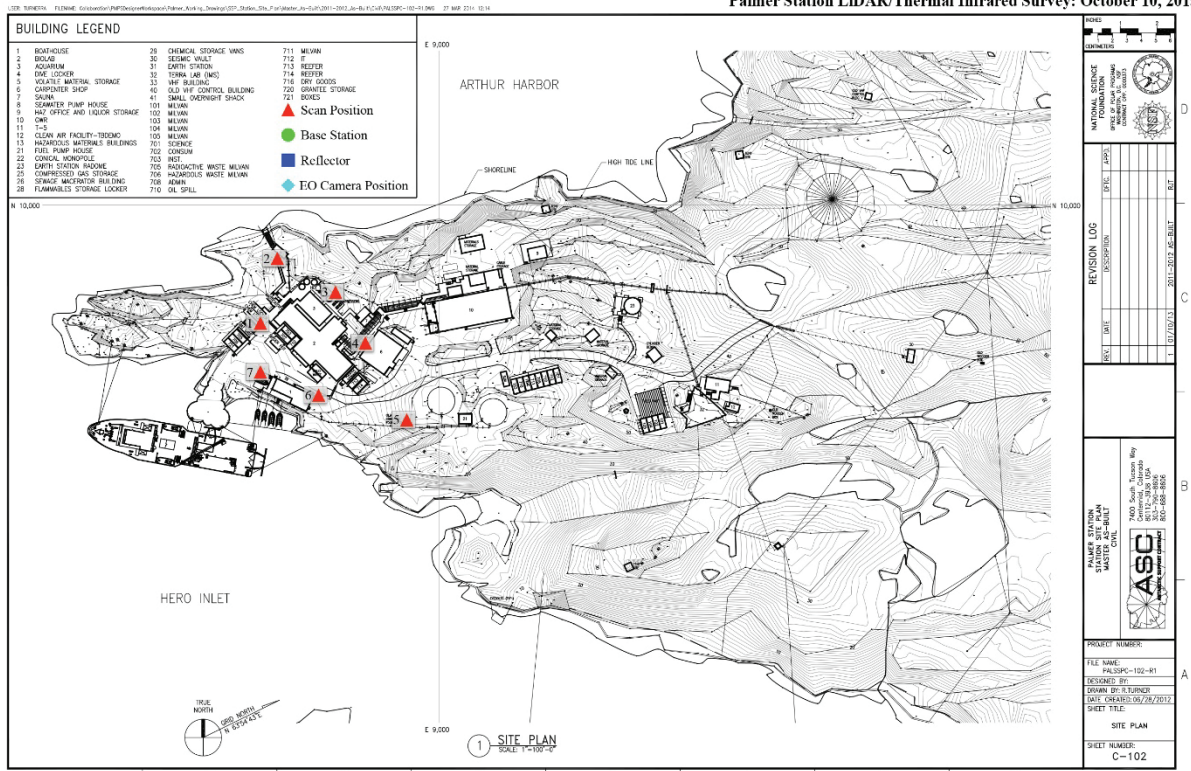
Appendix A: Palmer Survey Maps



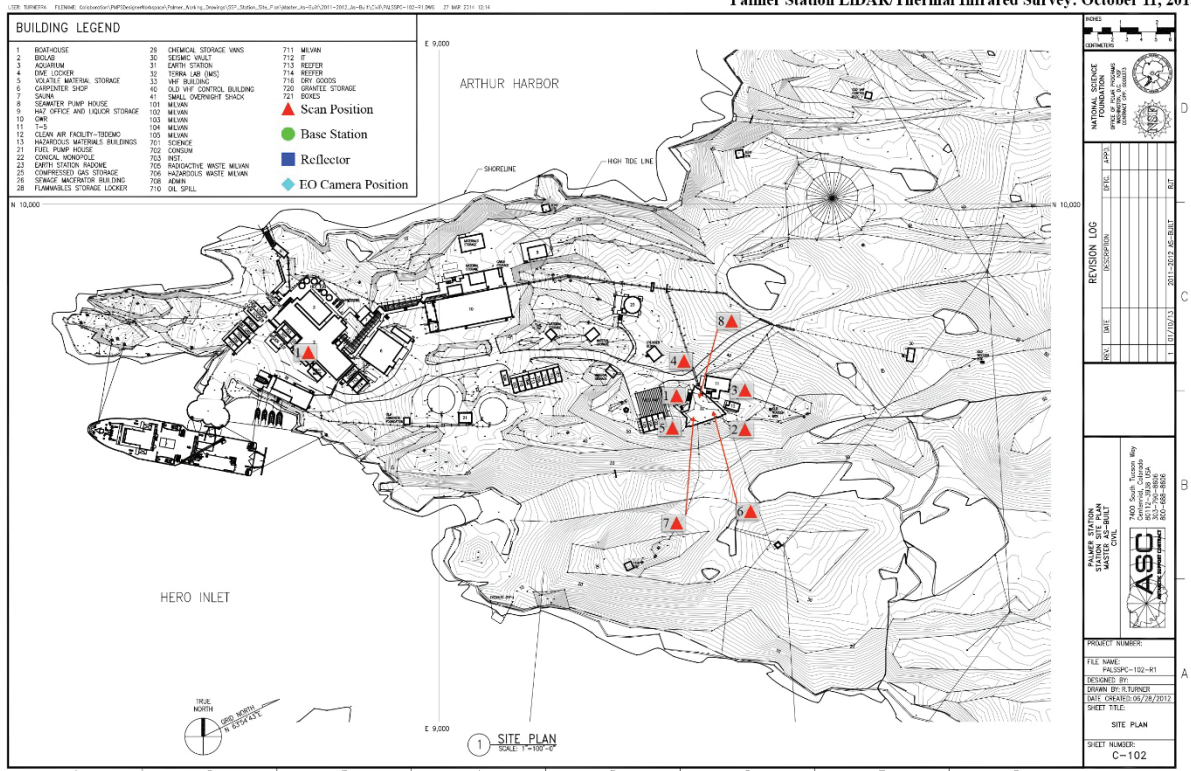
Palmer Station EO Camera Survey: October 10, 2015



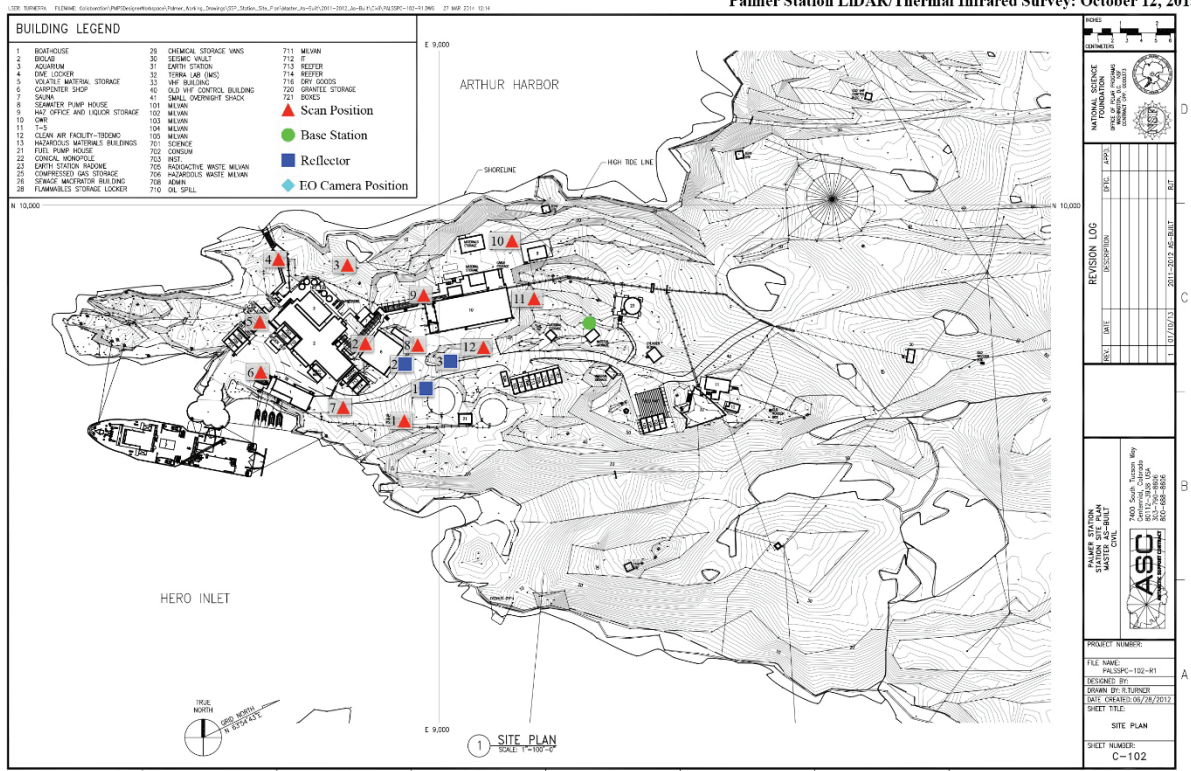
Palmer Station LiDAR/Thermal Infrared Survey: October 10, 2015



Palmer Station LiDAR/Thermal Infrared Survey: October 11, 2015



Palmer Station LiDAR/Thermal Infrared Survey: October 12, 2015



Appendix B: CRREL Lidar/TIR System Data Acquisition Procedure

January 2017, South Pole Station

B.1 Overview

This document describes the acquisition procedure for capturing coregistered thermal images using the InfraTec VarioCAM HD camera and Riegl VZ-1000 terrestrial laser scanner.

B.2 Acquisition PC setup

B.2.1 Network

1. Set LAN networks connection to the following settings:
 - a. IP address: 192.168.2.2
 - b. Subnet mask: 255.255.255.0
2. Ensure RiSCAN Pro (RSP) and IRBIS 3 Professional is installed
3. When scanner is powered, select the Wi-Fi S9998518, password 123456789.
4. Connect InfraTec Ethernet cable to laptop, and check connection via cmd if necessary.

B.2.2 RiSCAN Pro setup

1. Create a new project.
2. In the project attributes, set the following:
 - a. Instrument Tab, Scanner IP: 10.0.0.1 (if using wireless) 192.168.2.125 (if using network cable. Note that this was changed to work with the InfraTec address.)
 - b. Camera model: Custom camera
3. Set image acquisition to external software:
 - a. Tools>Options>Image acquisition
 - b. Image acquisition controlled by: Software
4. Set Camera and Mounting calibrations
 - a. Camera: Result calibration nikonD700_2505549_20mm_Final_4256x2832
 - b. Mounting: Result mounting nikonD700_2505549_20mm_Final

B.2.3 InfraTec IRBIS 3 Professional setup

1. Camera IP address is preset to 192.168.2.15
2. Open IRBIS 3 Professional.
3. Ensure that the scanner is powered and the camera is initialized.
4. In Camera tab, select “Connect.”
5. Use VarioCAM HD; the camera will connect and display a live image.
6. Select the “Remote” tab to display the focus options.
7. Go to the “View” tab.
8. Select the “Scale” tab.
9. Return to the “Camera” tab.
10. Use the “Live” tab to see a live view.
11. In the “Snap” tab, ensure it is set to “Premium and Auto save.”

B.3 Hardware setup

1. Attach the scanner to the survey tripod.
2. Attach the InfraTec VarioCAM HD TIR camera to the scanner.

B.4 Collection of data

1. In RiSCAN Pro collect a scan with settings appropriate to the project, but do not acquire the images automatically.
2. After the scan is complete, right-click the scan and select “Image acquisition.” (If using the network cable with the scanner, switch project to wireless [10.0.0.1], disconnect scanner network cable, and connect the InfraTec network cable.)
3. Use the “NikonD700_2505549_20mm_Final Scanner” camera calibration/mounting file.
4. Use a 40% overlap to ensure good coverage of the scan area.
5. The scanner will move to the first image phi angle and prompt the user to capture the image.
6. Go into IRBIS 3 and focus the camera; then select “Snap,” and verify that the new image with naming convention YYYYMMDD_HHMMSS.irb was saved.
7. Back in RSP, select “OK” to proceed with the next image.
8. Proceed for all images.
9. End the scan position, and proceed to the next position.

Appendix C: Scanning Log—Reflector Survey

Palmer Station Survey Notes

Date	Scan Position	Focus Building	Scan Start Time (GMT)	Image Start Time (GMT)	Temp (C)	Relative Humidity (%)	Barometric Pressure (mbar)	Wind Speed (m/s)	Notes
2015/10/9	001	Biolab	1:27	1:46	-0.7	83.4	994.7	1.9	GPS may not be accurate; collect external GPS
	002	Biolab	2:15	2:41	-0.7	75.5	995.0	2.0	No additional reflectors
	003	Biolab	2:54	3:24	-2.1	85.6	994.8	2.1	No additional reflectors
	004	Biolab	4:29	4:41	-2.2	86.6	994.5	1.9	Snowing
	005	Biolab	5:52	N/A	-1.4	88.3	994.3	1.7	Snow/ice sticking to windows/lens; end of survey
2015/10/09 Interior (Optimal Conditions)	001	GWR	22:17	22:31	21.0	36.2	993.5	-	Interior Room 203, temperature with window open
	002	GWR	22:55	23:06	24.0	46.2	993.5	-	GWR garage
2015/10/10	003	GWR	0:11	0:29	1.2	88.6	993.8	1.0	Outside, thermal is noisy due to snowing + wet
	004	GWR	0:48	1:02	1.8	12.5	993.7	0.4	Wet, snowing
	005	GWR	1:17	1:29	0.1	92.9	993.4	4.0	Windy, sideways snow
	006	GWR	1:59	2:10	0.2	94.2	992.9	5.1	Windy, sideways snow
	007	GWR	2:26	-	0.2	95.2	992.3	3.7	Noticeable snow build up on window, end survey
2015/10/10	001	Biolab	16:58	17:09	2.4	71.8	989.1	3.0	Daytime scanning, so thermal may be suspect
	002	Biolab	17:23	17:34	2.6	70.6	989.5	4.0	Daytime scanning, so thermal may be suspect
	003	Biolab	17:43	17:55	1.2	83.8	989.8	3.7	Daytime scanning, so thermal may be suspect
	004	Biolab	18:05	18:16	2.1	82.6	989.4	1.4	Daytime scanning, so thermal may be suspect
	005	Biolab	19:29	19:40	1.4	86.4	989.5	2.6	Daytime scanning, so thermal may be suspect
	006	Biolab	19:54	20:05	1.2	85.9	990.0	2.1	Daytime scanning, so thermal may be suspect
	007	Biolab	20:13	20:24	0.8	88	989.7	4.7	Daytime scanning, so thermal may be suspect
2015/10/11 (Optimal Conditions)	001	Terralab	23:56	0:07	1.2	78.1	988.3	2.0	Started on 2015/10/10 @ 23:56. No precipitation, lights on outside
	002	Terralab	0:23	0:34	0.7	78.1	988.1	1.4	No precipitation, lights on outside
	003	Terralab	0:42	0:53	0.4	82.6	988.2	4.6	No precipitation, lights on outside
	004	Terralab	1:03	1:16	0.2	84.9	987.9	3.6	No precipitation, lights on outside
	005	Terralab	1:34	1:44	-0.2	90.9	987.4	3.4	Light graupel snow
	006	Terralab	2:26	2:46	18.1	87.1	987.1	-	Inside Terralab
	007	Terralab	2:54	3:02	19.0	75.2	987.2	-	Inside Terralab
	008	Terralab	3:09	3:19	20.8	41.2	987.1	-	Inside Terralab
2015/10/11 Interior (Optimal Conditions)	001	Biolab	15:59	-	20.9	25.4	992.7	-	Interior of Biolab (cafeteria)
2015/10/12 (Optimal Conditions)	001	Biolab	0:40	0:50	-2.6	66.5	992.1	1.2	Calm
	002	Biolab	1:01	1:14	-2.7	73.3	992.1	1.0	Calm
	003	Biolab	1:22	1:35	-0.6	72.3	992.2	0	Calm - Hot Tub!
	004	Biolab	1:46	1:57	-2.5	74.5	992.4	0	Calm
	005	Biolab	2:05	2:16	-3.3	71.4	992.5	0.8	Calm
	006	Biolab	2:23	2:33	-5.1	77.0	992.4	1.1	Calm
	007	Biolab	2:40	2:51	-4.4	76.8	992.2	1.0	Calm
	008	GWR	4:10	4:23	-3.1	70.5	991.6	1.7	Calm winds, no precipitation
	009	GWR	4:31	4:41	-2.2	69.8	991.7	1.4	Calm winds, no precipitation
	010	GWR	4:50	5:01	-3.9	69.1	91.8	1.1	Calm winds, no precipitation
	011	GWR	5:11	5:21	-3.2	79.6	991.7	1.5	Calm winds, no precipitation
	012	GWR	5:32	5:42	-2.3	76.1	992.0	1.3	Calm winds, no precipitation

Palmer Station 2015 LiDAR/TIR Ground Control Survey

Measurement	2015/10/10			2015/10/12		
	TP001	TP002	TP003	TP001	TP002	TP003
Latitude	64° 46' 27.40092" S	64° 46' 28.37823" S	64° 46' 27.25686" S	64° 46' 28.33009" S	64° 46' 27.32508" S	64° 46' 27.86385" S
Longitude	64° 03' 11.51934" W	64° 03' 12.07505" W	64° 03' 06.35987" W	64° 03' 11.92184" W	64° 03' 11.55693" W	64° 03' 10.48982" W
Height (WGS84)	24.703	23.770	31.255	24.201	24.759	25.695
Horizontal Precision (m)	0.005	0.006	0.005	0.004	0.007	0.004
Vertical Precision (m)	0.010	0.011	0.010	0.010	0.017	0.010
Satellite (min)	9	9	9	9	10	9
RDOP (max)	2.1	2.3	1.8	1.5	2.8	3.1
HDOP (max)	0.9	1.1	0.8	0.6	1.1	1.2
VDOP (max)	1.8	2.0	1.6	1.3	2.6	2.9
Positions Used	16	16	16	16	16	16
Start Local Date	2015/10/10	2015/10/10	2015/10/10	2015/10/12	2015/10/12	2015/10/12
Start Local Time	04:29:52	04:28:21	04:32:23	07:02:20	07:03:52	07:04:53
Stop Local Time	04:30:07	04:28:36	04:32:38	07:02:35	07:04:07	07:05:08
RMS	8.9	12.1	11.0	10.4	14.4	16.7
UTM Zone	20S	20S	20S	20S	20S	20S
Easting (m)	449917.700	449910.880	449985.811	449912.900	449917.185	449931.536
Northing (m)	2816284.882	2816254.562	2816290.472	2816256.044	2816287.214	2816270.845
Corrected Height (WGS84) (m)	24.6218	23.6888	31.1738	24.1198	24.6778	25.6138